A STUDY TO DETERMINE THE VALIDITY AND ACCURACY OF A LOW COST, WIDELY ACESSIBLE 3D FACIAL SCANNER COMPARED TO AN ESTABLISHED STEREPHOTOGRAMMETRY BASED SYSTEM.

by

KELLY THOMAS

A thesis submitted to the University of Birmingham for the degree of

MASTER OF SCIENCE BY RESEARCH

School of Dentistry

College of Medical and Dental Sciences

University of Birmingham

July 2023

ACKNOWLEDGMENTS

I would like to express my deepest appreciation and thanks to Professor Khambay, he has been unwaveringly patient, kind and knowledgeable throughout my training. This project would not have been possible without his generous help and support.

I would like to thank my colleagues at the Birmingham Dental Hospital for agreeing to take part in this project and their encouragement to get to the finish line.

I would like to both apologise to and thank my family, Bea and Teleri for being somewhat absent recently and for their support of my studies over the last decade.

ABSTRACT

AIMS

The aims of the in vitro study were to determine the validity and accuracy of two Bellus3D devices - Bellus3D Face Camera Pro (Android device) and Bellus3D and iPhone 12 (Apple device), and two commercial 3D facial imaging systems - 3dMD and Di4D SNAP. The aims of the in vivo study were to determine the validity and accuracy of Bellus3D Face Camera Pro (Android device) compared to Di4D SNAP whilst capturing the face at rest and at maximum smile.

MATERIALS AND METHODS

For the in vitro study a plastic mannequin head was pre-marked with 35 facial landmarks and the 3D coordinates of each of the landmarks was found using a coordinate measuring machine (CMM). This produced the gold standard 3D configuration. The head was also scanned using four three-dimensional imaging systems i.e., Bellus3D Face Camera Pro (Android), Bellus3D Application (app) and iPhone 12, 3dMD and Di4D SNAP. For each device the image was digitised on-screen. The 3D landmarks configuration for each device was compared to the gold standard CMM data following partial Procrustes superimposition. The Euclidean distance between the landmark pairs was measured as well as mean absolute difference in the x, y and z-directions.

For the in vivo study 21 landmarks were placed directly on the faces of 30 volunteers meeting the inclusion criteria. Participants rehearsed rest position and maximum smile. For each participant images were captured at rest and maximum smile, using the Bellus3D Face Camera Pro and Di4D system. The images were digitised and both the 3D landmark configurations at rest were aligned using a partial Procrustes superimposition, this was repeated for both 3D landmark configurations at maximum

smile. The Euclidean distance and the mean absolute difference in the x, y and z direction between each landmark pair identified, a threshold of 2.0mm difference was set as being clinically significant different. Systematic and random error was assessed. Repeatability of rest position was also assessed.

RESULTS

For the in vitro study a two-sample Students *t*-test showed the mean difference in Euclidean distance (0.9 ± 1.4mm) between the Bellus3D devices and the commercial systems was statistically significant (p = 0.001) with a 95% confidence interval for the difference of -1.4mm to -0.4mm).

For the in vivo study, images taken by Bellus3D Face Camera Pro and Di4D at rest, showed that 18 of 21 extracted landmark pairs had a mean Euclidean distance of less than 2.0mm. Three landmark pairs; right and left gonion and menton were outside of the clinical level of acceptability (>2.0mm). The smallest differences were seen in landmarks located close to the midline of the face. For maximum smile, an additional 4 landmark pairs showed a mean Euclidean distance of greater than 2.0mm. These were right and left exocanthion and right and left cheilion.

CONCLUSIONS

The difference in accuracy and precision between the systems is most evident in the lateral and inferior landmarks because of the centralised camera location of the Bellus3D Face Camera Pro system and the need for subject rotation. Further reduction in accuracy was observed in maximum smile as the longer scanning time of the Bellus3D system captured involuntary changes in micro expression. Bellus3D Face Camera Pro is suitable for clinical application if limited to areas adjacent to the midline in rest position. Bellus3D Face Camera Pro is not suitable for clinical use where

investigation of lateral and inferior areas of the face is required, nor for transverse smile investigation.

LIST OF FIGURES

LIST OF TABLES

CONTENTS

CHAPTER 1

LITERATURE REVIEW

1.1 INTRODUCTION

Three-dimensional (3D) imaging has evolved rapidly over the last 30 years due to demands in fields such as manufacturing, engineering, and entertainment, combined with the facilitative advancement in technology. No longer restricted to specialist use, for reasons of hardware and cost, anyone with a smartphone is now able to create a 3D facial image. The purpose of this project is initially to familiarise the reader with the current state of the evidence regarding the use of 3D imaging within medicine and dentistry and to discuss the systems available. The experimental section will endeavour to determine if a widely accessible 3D imaging app is comparable to a commercial surface imaging system for 3D facial imaging and whether it could be used as an alternative in clinical situations, significantly reducing cost and hardware demands.

1.2 MEDICAL USES OF FACIAL THREE-DIMENSIONAL IMAGING

Three-dimensional facial imaging has found many applications in medicine and dentistry, these have included in normative databases (Smith *et al.*, 2021), surgical planning (Khambay *et al.*, 2002), longitudinal facial changes and as an outcome tool (Wampfler and Gkantidis, 2022).

1.2.1 Normative databases

Facial three-dimensional images have been used to create a database of normal cohorts in terms of facial growth, proportions, and symmetry (Smith *et al.*, 2021). These images can be used as a reference tool for identification of diseases and to assess treatment outcomes. It is necessary to identify normality across different races, sexes, and ages to allow comparative analysis. For instance, with regards to head and face

symmetry, a study quantifying normal craniofacial form based on over 500 North American children (0-18 years) found a mean head asymmetry of 1.5mm and a mean facial asymmetry of 1.2mm, with no significant differences seen in age, sex or race (Cho *et al.,* 2018). In a population of Taiwanese children (6-12 years), the average head asymmetry was 2.5mm and facial asymmetry was 1.0mm with no significant difference between genders (Hsu *et al.*, 2019). Whilst in a study of white Australian adults, females were generally more symmetric than males. Moderate asymmetry (2-5mm) was noted in over half of the participants (53% females and 58% males) and severe asymmetry (>5mm) affected 7% females and 8% of males (Lum *et al.*, 2020). These studies show there is a "normal' baseline craniofacial asymmetry in the population.

Given the 3D nature of mandibular asymmetry, 3D facial scans have been used to assess the influence of chin asymmetry on perceived facial aesthetics between orthodontists, dentists, and laypeople, and provide a quantitative reference for clinical intervention (Dong *et al.*, 2020). The study concluded that orthodontists and dentists were able to detect a chin asymmetry of between 2-4mm while laypeople did not detect chin asymmetries until they were greater than 4mm. This information can be used to rationalise conservative treatment for mild asymmetries.

1.2.2 Longitudinal facial changes

Sequential 3D facial imaging can be used as a means of monitoring gradual changes over time, such as ageing or disease progression. In order to obtain an accurate comparison, the images need to be superimposed on stable structures. A recent systematic review found that surface based superimposition methods were used most

commonly with the forehead being preferred due to its stability over time (Wampfler and Gkantidis, 2022). Stable structure identification can be difficult in growing patients; therefore it is also possible, in some instances, for the patient to serve as their own control in the current time point by creating a mirrored virtual patient to compare against (ter Horst, *et al.,* 2022). A recent study of infant (0-2 years) cranial growth obtained quarterly 3D scans of 130 subjects to produce detailed regional growth maps at different stages of development (Meulstee *et al.*, 2020).

1.2.3 Surgical planning

For the purposes of surgical planning CBCT hard tissue scans can be fused with 3D surface scans to produce a “virtual patient” (Khambay *et al.*, 2002). From an orthognathic surgery perspective this allows more accurate planning especially for complex asymmetry cases as it provides the surgical team with the visual information of moving the osteotomized segments with six degrees of freedom. In addition, it provides the patient with a visual outcome of the facial appearance in 3D. This addresses the inadequacies of using conventional profile photo-cephalometric techniques which are unable to depict the frontal view. This technology can also be used in the production of surgical stents and prosthetics led by the end facial result which is often the patients primary concern (Wang *et al.*, 2022). Crucially, by giving the patient a realistic outcome prediction, informed consent is improved significantly. Since this technology is readily available and should be standard in a secondary care setting where such treatment is planned, it would now seem inappropriate not to provide this information to a patient prior to surgery.

For instance, it is commonly accepted that a negative consequence of maxillary advancement are changes in the nasal soft tissue. Previous studies have confirmed widening of alar base, increase in alar width, nostril width, as well as nasal tip columella and upper lip projection (Ubaya *et al.,* 2012; Metzler *et al.*, 2014). This information allows for appropriate warnings and discussions to take place prior to treatment. It has previously been reported that following bimaxillary surgery, facial symmetry worsened post operatively, particularly at the nasal tip and chin prominence (Hajeer *et al.,* 2004).

In addition to surgical planning facial prosthesis construction has benefitted from the introduction of 3D surface imaging. Facial prostheses are traditionally made using impression materials to create a cast of the defect for the technician to work on. This is uncomfortable, messy and time consuming, and impression materials can be subject to shrinkage, air blows and voids (Beri *et al.*, 2022). It is now possible using 3D imaging and multi-modal imaging to create a digital cast, and a simpler and cleaner method of prosthesis fabrication using CAD-CAM technology and 3D printing (Jablonski *et al.,* 2019).

1.2.4 Cleft lip and Palate

Congenital craniofacial defects frequently require early correction to allow for growth, function and aesthetics. Cleft lip and palate is the most common of these disorders and there are many studies detailing the use 3D surface scans to assess outcomes in this population (Thierens *et al.*, 2018). Three-dimensional facial images have been used to objectively assess the symmetry of primary lip repair pre and post-surgery. Positive changes were found not only in the upper lip but in the nose and cheek area also (Al-Rudainy *et al.*, 2018). Medical treatment is ideally evidence based where

possible, for example naso-alveolar moulding prior to cheiloplasty surgery is a significant and protracted intervention that requires a substantial commitment from caregivers. It is important therefore to establish whether the intervention offers additional long-term benefit to nasal aesthetics compared to surgery alone. Three-dimensional surface scans offer an objective and quantifiable means of outcome assessment. In a comparison of scans taken at 5 years of age, the naso-alveolar moulding and surgery group displayed improved aesthetic outcomes compared to the surgery alone group (Kurnik *et al.*, 2021). Similarly, 3D surface scans have been used to identify which surgical technique produces better outcomes in a group of cleft patients. In a comparison study of philtral reconstruction techniques (overlapping mattress suture or asymmetric mattress suture) superior outcomes i.e. improved column symmetry and projection, were observed in overlapping mattress suture group (Chang *et al.*, 2020). For both clinicians and patients, it is important to assess the outcome of treatment to establish if the desired effects have been achieved but also to identify non-desirable effects and relapse potential so that these can be predicted and consented for pre-treatment.

1.2.5 Orthodontic treatment

The soft tissue effects of conventional orthodontic treatment have been assessed with 3D surface imaging. The consequence of extractions on facial profile is contentious and has previously been assessed using two dimensional (2D) lateral cephalograms (Freitas *et al.*, 2019). A recent study has used 3D imaging and found that extraction treatment in adult females negatively affected nasolabial folds and lip projection (Zhou *et al.*, 2023). In addition an increase in naso-labial angle has been reported in the extraction group (Rongo *et al.*, 2021). In a society that is increasingly concerned with

facial aesthetics these may be potentially serious side effect of treatment that the patient should be informed of during the consent process.

Functional appliances have been shown to produce skeletal and dental changes in a growing patient; however, it is likely that the soft tissue changes are of greater importance to the patient. A comparison of soft tissue outcomes of treatment with three removable functional appliances, Twinblock, Herbst and monoblock appliances, found that all had a positive effect on the profile by increasing the angle of convexity (Güler and Malkoç, 2020). An investigation of soft tissue changes post treatment with a fixed functional (Class II corrector - Forsus™ spring) displayed no statistically significant changes to the pre-treatment soft tissue. (Akan and Veli, 2020).

In a recent development, three dimensional facial scans have recently been used to design customised facemasks in situations where an improved fit is necessary e.g. for nenonates requiring ventilation masks (Bockstedte *et al.*, 2022) or in the recent COVID-19 pandemic where a tight seal was necessary to prevent transmission of vaporised virus (Carter *et al.,* 2021).

The use of 3D surface facial scanning offers advantages over conventional 2D methods by reducing distortion and generating supplemental information which obviates the need for direct anthropometry. In addition, the 3D surface scanning can be non-invasive and involves no ionising radiation. The speed of scanning time makes this a practical and reliable method of recording the cranial and facial features of young children. Ritschl et al. (2018) used a low cost portable stereophotogrammetry system (FUEL3D® SCANIFY®) to scan a neonatal population monthly from birth to 6 months.

The scans were well tolerated and accurate (within 1mm) compared to conventional plaster models and easier to obtain (Ritschl *et al.*, 2018). Once captured digital storage of the raw images permits easy recall and re-analysis as required.

1.3 3D IMAGING

3D investigation of subdermal tissues is well established within medicine having been used since the late 1970's (Bird, 1982). Various imaging modalities have been developed to facilitate the examination of individual tissue types, often developed from pre-existing two-dimensional (2D) systems. The following is a compendious summary of current 3D medical and, more specifically head and neck imaging systems. These can be divided into those methods that image volume and those that capture the surface only. From a facial imaging perspective, volumetric imaging captures the internal structures of the head and neck, whilst surface imaging captures the air / soft tissue boundary.

1.4 3D VOLUME CAPTURE

1.4.1 Computed tomography (CT)

Biological hard tissues are conventionally imaged using x-ray beams, their relative absorption or reflection conveying a representation of the underlying structures. In their most basic form radiographs are a 2D image of the area overlying the sensor, with no representation of depth. Within head and neck imaging, the advent of focal plane tomography enabled 2D imaging of a curved structure i.e., the midface. It consists of the simultaneous movement of an x-ray beam and film around the structure of interest, which therefore remains in focus throughout the exposure, the resultant image being a composite of the multiple capture points. 3D radiographic imaging is produced in a

similar way; numerous images, known as “slices”, are taken in multiple planes around a subject and digitally stitched together, or volume rendered, to form a 3D representation. CT scans are interactive and crucially, give the clinician an appreciation of depth, they are used extensively in oral and maxillofacial surgery. Obviously, due to the increased capture points required the exposure of the patient is amplified from approximately 0.010 mSv, in a standard dental panoramic tomograph (DPT), to 2.1 mSv in a maxillary-mandibular CT scan (Ngan *et al.*, 2003).

Conventional CT scans offer a rudimentary representation of the soft tissues; volume and outline can easily be appreciated, whilst differentiation is poor. In comparison hard tissues are well demarcated. Cone beam computed tomography (CBCT) is a further development aimed at reducing exposure; the x-ray beam is cone-shaped rather than fan-shaped. This allows imaging of a smaller more focused irradiation field; ranging from a few cm^3 to both jaws, in a single scan (Machado, 2015). This technique is valuable in dental surgery and oral medicine where a localised field of view is sufficient. CBCT combined with DPT machines are now available as a single unit and are no longer the domain of specialised centres or secondary care as with conventional CT.

1.4.2 Magnetic Resonance Image (MRI)

The gold standard for soft tissue 3D imaging is Magnetic Resonance Imaging (MRI). Unlike CT it is capable of excellent soft tissue differentiation as it depends not on the relative mineral density of the tissue but the relative de-excitation of hydrogen ions readily found in the water content of soft tissue (van der Heide *et al.*, 2019). This is achieved by application of a strong magnet which causes a uniform spin alignment of the hydrogen ions, combined with a radio frequency current. Once the magnet is

deactivated the hydrogen ions return to their normal spin emitting a radio signal as they do so. The strength of the signal recorded by a sensor is used to create a representative image of the tissues, which as for CT scans, is interactive and can be viewed as a 3D reconstruction or as 2D slices. MRI, like CT is highly specialised and subject to similar disadvantages in terms of cost and accessibility. It is also incompatible with ferric containing metal implants and, being relatively slow to capture is sensitive to motion artefact (Zammit-Maempel, 2015). The main advantage of MRI is that it does not utilise ionising radiation.

1.4.3 Ultrasound Imaging

A more accessible, albeit cruder method of soft tissue imaging is ultrasound scanning. Ultrasound systems emit high frequency soundwaves into the tissues via a transducer placed over the tissue surface. The soundwaves are reflected to varying degrees dependent on a tissue's density and distance from the source. The echoes detected by the transducer are converted into a representative real-time image of the underlying structures. Consequently, ultrasound has applications in functional imaging such as joint movement, activity of vital organs, obstetrics, and fine needle aspiration biopsies as well as primary visualisation, often being used for investigation of neck masses (Carter *et al.,* 2017). 3D ultrasound requires the application of soundwaves at multiple angles and surface rendering of the image, if done in real time then the scan is, in essence 4D (Carter *et al.,* 2017). The use of 3D ultrasound in the maxillofacial region has been of limited value due to the difficulties in capturing the air / soft tissue boundary without distorting the soft tissue (Hell, 1995).

1.5 3D SURFACE CAPTURE

Currently, surface imaging within medicine and dentistry relies on conventional two-dimensional photographs. These may be sufficient in some cases, dependent on the indication however, a 2D image cannot reliably represent a 3D structure, and 2D images are subject to distortion and perspective errors (Lane and Harrell, 2008; Dindaroğlu *et al.*, 2016). The use of 3D surface imaging of the face within medicine and dentistry is not well established or routine practise in dentistry, yet it has had the potential to improve diagnosis, treatment, and disease monitoring.

An ideal facial imaging system would need to capture topographic, texture, and colour information, be non-invasive, rapid, accurate, precise, portable, and inexpensive. 3D surface images are typically created by “reverse engineering”. The process uses an imaging device to take a physical object, in this case a face, and turn it into a digital model based on “point-cloud data”. Each point or vertex has x, y, z co-ordinates which are joined to form a mesh, to which surface texture and colour information is added (Lane and Harrell, 2008). Thus, 3D imaging offers the potential to extract the three-dimensional co-ordinate data for any landmark (Lane and Harrell, 2008).

For an imaging system to be valid it must be accurate and precise (Lane and Harrell, 2008). With regards to the current literature, accuracy is the agreement of the experimental measurement against a true measurement or gold standard. Previous studies have established the level of accuracy acceptable for clinical application of 3D facial scans to be within 2mm (Aung *et al.*, 1995; Kovacs *et al.*, 2006; Knoops *et al.*, 2017). Precision can be sub-divided into repeatability and reproducibly. Repeatability is a measure of the degree of consistency between repeated measures of the same

subject, using the same technique. This includes operator error i.e., inconsistency when the same operator is extracting the same data from the same set multiple times; and system error i.e. inconsistency when scanning the same subject under the same conditions multiple times (Lübbers *et al*., 2010). Reproducibility is the inconsistency between repeated measurements of the same subject using the same technique but between operators.

1.6 STRUCTURED LIGHT

Structured-light scanners work by projecting a light pattern on the subject face and using sensors or cameras to detect the deformation of the pattern. An algorithm determines distance of the deformation points from the light source and the data is reverse engineered into an image of the physical object. These systems are sensitive to ambient light and work best in an environment with consistent controlled lighting. Scan time is variable depending on the system but can take up to 30 seconds. Surface texture and colour is often added to the final image. Light based systems also have simple hardware requirements, needing only a light source, sensor and processing unit. Contemporary systems use dual structured light with infra-red sensors and are typically manufactured as handheld single units containing the light source and the sensor.

Ma et al. (2009) validated a novel structured light facial scanning system (BWHX Technology Company, Beijing, China) (Ma *et al.,* 2009). The system under investigation was designed to reduce motion error by incorporating a mirror into the set up so that neither the subject nor the sensor required moving between scans. Although two separate captures were needed, the speed at which they could be

acquired was reduced to 5 seconds. Accuracy and precision were investigated under ideal conditions using a facial plaster cast that had 19 landmarks. Experimental system landmark co-ordinates were compared to those derived from a co-ordinate measuring machine. The accuracy was found to be 0.93 ± 0.36mm, two landmarks; trichion and sub-nasale, showed a difference of more than 1mm and were potentially affected by reflection and shadowing respectively. Reproducibility was determined by comparing landmarking of scans between investigators and found to be 0.79 ± 0.36mm. Surface-to-surface analysis showed a mean difference between the scans of 0.20mm indicating that the system is reliable to clinically acceptable levels (Ma *et al.,* 2009).

1.6.1 Moirè

Moirè topography is a form of structured light scanning developed in the 1970's using the Moirè phenomenon. The Moirè phenomenon exists when two standardised patterns of curves or circles overlap, if projected onto an uneven surface, new patterns are created, distinguishing the depths of the surface (Porto *et al.*, 2010). The main medical application is to identify asymmetries, particularly those of gait associated with scoliosis (Porto *et al.*, 2010). Within the head and neck region previous uses have included assessment of facial deformity following zygomatic injury and quantification of facial palsy (Kawano, 1987; Yuen, *et al.*,1997).

Dirckx et al. (2010) introduced a new technique based on the Moirè phenomenon - Projection Moirè Topography (PMT). PMT was designed to reduce the time taken for image capture, from several seconds to approximately 1 second (Dirckx *et al.,* 2010). Twenty-two 3D printed photopolymer models were constructed from anonymised CT data and scanned using both the experimental system and Di3D. The resultant 3D

scans was superimposed onto original segmented soft tissue CT scan, and heat maps generated to illustrate the difference (Artopoulos *et al.*, 2014). The Moirè system showed a 95.1% concordance with the CT scan compared to a stereophotogrammetry imaging system (Di3D), which showed a 98.6% agreement. It was noted that the Moirè method performed less well toward the lateral boarders of the face, possibly due to the distortion when using a single camera system. The authors concluded that in vitro the techniques are comparable in accuracy and plan to repeat the study in vivo.

1.7 STEREOPHOTOGRAMMETRY

Stereophotogrammetry utilises camera pairs to capture images of an object. The cameras are located at a known distance and angulation to one another. Using the principle of triangulation, and the appropriate calibration, the software system uses the captured images to generate a polygonal 3D mesh of the face. The polygonal mesh is then made “photorealistic” by the addition of the captured texture and colour information. Capture between all the cameras must be synchronised or else there is a risk of discrepancy between all the images. The process of image capture is rapid and is determined by the camera aperture speed, and this can be as fast as 1/500 (2ms) (Lane and Harrell, 2008).

While less sensitive to ambient light than the other systems, due to the use of flash-light, stereophotogrammetry has difficulties capturing reflective surfaces; hair, teeth, facial jewellery and oily skin as the glare produced by the flashes causes data loss (Heike et al., 2010). Areas that are subject to “loss of line of sight” (undercuts and shadowing) are similarly affected, for example sub-nasal and submental areas (Heike *et al.,* 2010). Tilting the head upwards can reduce shadowing, although for

reproducibility purposes, facial capture in natural head position is frequently sought. It is possible to fuse overlay the 3D surface images captured with CT or CBCT data to produce a comprehensive hard and soft tissue virtual patient (Khambay *et al.,* 2002). Conventional stereophotogrammetry systems are generally cumbersome, expensive and require daily calibration (van Loon *et al.,* 2010).

Stereophotogrammetry systems can be passive or active. Active systems project an additional specked infra-red image over the face; whilst the passive systems use the skin pores and texture for triangulation (Lane and Harrell, 2008). The Di3D and more recent Di4D SNAP systems (Dimensional Imaging, Glasgow, UK) are passive stereophotogrammetry systems, which use 3 pairs of cameras, producing six coloured images. These images and irregularities in skin texture, together with the calibration data, are used to construct a 3D photo-realistic image. The 3dMDface™ system (3dMD LLC, Atlanta, USA) is an active stereophotogrammetry system which also uses 6 cameras to take 3 pairs of photographs simultaneously in 1.5ms. Two pairs of images are taken with infrared cameras with an overlying specked light pattern projection, the final pair of images are taken in colour and when combined with the calibration data and speckled images to produce a 3D photo-realistic image (van Loon *et al.*, 2010).

1.7.1 In vitro validation

An in vitro validation study of the Di3D system showed that with regards to reliability of mannequin head capture, there was a mean system error of 0.057mm (the mean difference of 10 repeated exposures compared with the mean surface) (Winder *et al.,* 2008). Errors up to 1.06mm were found at the extremities of the facial image, errors in midline measurements were reported to be associated with areas of shadowing i.e.

under the chin and near the inner canthus (Winder *et al.*, 2008). The mean difference of 20 pre-marked linear distances, between Di3D captured images and those recorded directly from the mannequin head using digital callipers, was 0.62mm, with a maximum and minimum error of 1.43mm and 0.06mm, respectively.

A similar study was conducted using the 3dMD System, the mean system error was found to be 0.2mm (Lübbers *et al.*, 2010). The mannequin head was pre-marked with 41 landmarks and 201 linear distances were measured using direct anthropometric techniques and compared to those derived from the 3dMD captured image. The mean error was 0.01 ± 0.55mm, with all differences reported as statistically insignificant. These investigations were conducted under ideal conditions with any subject movement eliminated. The results provide a baseline level of error, as it would be anticipated that measurements on live subjects would be similar or worse. It is worth noting that both studies reported on differences in linear measures, however errors in a linear distance can be a result of the error landmark endpoints. The use of linear measurements (Euclidean distances) is historically clinically routine but has a major shortcoming in that it provides a measure of length only and no indication of direction.

1.7.2 In vivo validation

The in vivo precision of the 3dMD system was investigated using a sample of 8 participants and two operators, identifying 27 landmarks (Nord *et al.*, 2015). The study reported no statistically significant differences in inter-examiner repeatability or intra-examiner reproducibility. Landmarks were grouped according to those that could be identified with high, medium, and low precision; however no numerical values were given. Landmarks located around the mouth could be identified with higher precision,

whilst lateral landmarks (gonion) and in areas of shadowing (subnasale) had the lowest precision. Aldridge et al. (2005) used a representative sample of individuals, including children with craniofacial syndromes, to investigate the repeatability of 3dMD (Aldridge *et al.*, 2005). The study found 3dMD to be precise in the repeated identification of landmarks (6 midline and 7 bilateral) even without pre-landmarking the subjects, with 14 of the 20 landmarks showing concordance within 1mm (mean 0.827mm, range 0.17 to 4.10mm). Again, the greatest error was found in the gonial region.

Dindaroğlu et al. (2016) compared direct facial measurements to 3dMD scan measurements of 80 participants (Dindaroğlu *et al.*, 2016). Despite no pre-landmarking, the greatest mean difference between the linear measurements was 0.21mm, however only 10 measurements were compared. Wong et al. (2008), in an earlier study, compared 18 linear measurements (10 midline and 8 bilateral) using direct facial measurements to 3dMD scan methods in 20 un-landmarked patients (Wong *et al.*, 2008). Fifteen of the 18 linear measurements were within 1mm, the largest error was found in lateral measurements (tragus to gonion) Repeatability was superior for 3dMD than direct measurement (average error of 0.8mm, compared to 1.0mm). Both methods were equally precise for operator repeatability (correlation coefficient of 0.91 for 3dMD and 0.90 for direct measurement).

Previous studies have shown that stereophotogrammetry systems are in general as accurate and precise as direct anthropometric measurements, within the 2mm level of clinical acceptability. None of the in vivo studies discussed above pre-landmarked the subjects. The precision of landmark identification could be adversely affected if identification was usually aided with palpation of underlying bony structures (Nord *et*

al., 2015) or if the landmarks were more laterally located (Aldridge *et al.*, 2005). Similar times were reported to perform direct and digital anthropometry, averaging approximately 30 minutes per individual (Wong *et al.*, 2008). The advantage of stereophotogrammetry is that once the subject has been imaged a digital record has been saved and can be viewed or re-analysed if necessary.

1.7.3 Portable stereophotogrammetry

Whilst stereophotogrammetry has been shown to have excellent accuracy and precision, the systems are largely expensive and cumbersome. Portable stereophotogrammetry systems were developed in the hope of overcoming these issues. Vectra H1 (Canfield Scientific, Parsippany, NJ, USA) is a single camera portable system that costs approximately a third of the of Di3D system. It has a mirror incorporated into the lens that allows the capture of two images simultaneously. For ear to ear imaging the manufacturer recommends taking 3 scans at different angles, giving a total of 3 paired images as per the traditional stereophotogrammetry systems. The capture time is 2ms and flash recharge is 5 seconds therefore the whole process takes approximately 10 seconds. The images are merged in the software package to create the final 3D image.

In a comparison study of Vectra H1 to 3dMD, Camison et al. (2018) used a pre-landmarked mannequin head to investigate the differences between the two facial images, using surface-to-surface measurements (Camison *et al.*, 2018). The mean global RMS error under ideal conditions, was 0.144mm. Repeatability of the Vectra H1 system between two identical mannequin head scans was 0.034mm on average. The in vivo study compared the scans of 23 subjects, who had been pre-landmarked with

17 landmarks, generating 136 linear measurements. The mean technical error of measurement (MTE) between the two imaging systems, was 0.84mm (range 0.19 – 1.54mm), the highest errors were found in the lateral regions of the face and lowest error was toward the facial midline. In a comparison of surface-to-surface measurements, the average RMS global error was 0.43 mm (range 0.33–0.59mm). The results show Vectra H1 to be valid and precise in an ideal in vitro environment. The increase in error in vivo is still within the limit of clinical acceptability and is likely due to subject movement, given the relatively long scanning time of 10 seconds. Indeed, the largest error was around the corners of the mouth and the eyelids which is consistent with changes in micro-expression. A recent systematic review has reported that Canfield's Vectra imaging systems (Vectra M5, M3, XT and H1) are all capable of capturing precise and reproducible 3D facial images, with some imprecisions reported around the perioral region (De Stefani et al., 2022). Any errors are likely to be compounded if these systems are used in less compliant samples, for example children or those with learning difficulties and reinforces the importance of sub-second capture time to the validity of a surface imaging system intended for in vivo use.

1.8 LASER

Laser based scanning systems were developed in the early 90's and originated in the engineering industry. A laser beam or stripe is projected over the surface of an object and its deflection is recorded by a sensor at a known triangulation point (angulation and distance) from the laser source, allowing for trigonometric determination of the objects x, y and z co-ordinates (Lane and Harrell, 2008; Karatas and Toy, 2014). These systems are reasonably simple in their setup and hardware demands, and as such more portable and economical than stereophotogrammetry. Their principal drawback

is that there is a long scanning time of up to 30 seconds and while not problematic for engineering purposes, presents a challenge for facial imaging as the subject needs to remain motionless for the entire capture time or else risk motion error (Ayoub *et al*., 1998; Karatas and Toy, 2014; Gwilliam *et al*., 2006). Other drawbacks include concerns over safety of laser exposure to the eyes (Karatas and Toy, 2014) and lack of surface texture and colour application to aid landmark identification and create a relatable image for patient consent (Gwilliam *et al*.,2006; Artopoulos *et al.*, 2014; Karatas and Toy, 2014). These issues have largely been overcome with the newer generation of laser scanners which are safe for eyes and able to capture texture and colour with the incorporation of a camera into the set up.

1.8.1 In vitro validation

An in vitro experiment using the Minolta Vivid700 3D laser surface scanner compared 21 linear measurements derived from pre landmarked facial plaster casts to those from direct measurement. 12 landmarks were placed, none of which were at the extreme edges of the face. The casts were scanned from three different views and the data merged post capture using the Vivid software. The average difference between the measurements was 1.9mm ± 0.8mm (Kusnoto *et al*., 2002). A similar study comparing linear measurements of 19 nasal plaster casts using both the laser based Dental Wings series 3 scanner (Dental Wings Inc., Montreal, Canada) and the Vectra stereophotogrammetry system (Vectra 3D, Canfield Scientific, Fairfield, NJ) found no significant differences in outcome measures (Codari *et al.*, 2015). Unfortunately, the study lacked detail and should be viewed with caution.

1.8.2 In vivo validation

The Minolta Vivid 910® (Minolta Co., Ltd., Osaka, Japan) is eye safe and patients can be scanned with their eyes open. Ear to ear capture requires movement of the scanner, the subject, or the addition of a second sensor. Kovacs et al. (2006) investigated the precision and accuracy of the scanning system with comparison to direct anthropometrical measurements in five pre-landmarked subjects (Kovacs *et al.*, 2006). The experimental capture involved either automated subject rotation taking 90 seconds; manual subject rotation over a 45 second period, or a dual-sensor static subject capture taking 10 seconds. Repeatability and reproducibility were highest in the static capture method, followed by manual rotation method, and then automated rotation, indicating that capture time had a great influence on precision. The composite 3D images were land-marked and linear distances compared to direct clinical measurements. Overall, the mean differences in distances between the clinical measurements and the facial laser scans were 1.32 ± 5.67mm.

A more recent comparison of the Minolta Vivid 910® scanner to the Vectra M3 system (VECTRA-3D®: Canfield Scientific, Inc., Fairfield, NJ, USA) used 15 participants. (Gibelli *et al.*, 2018). A tri-capture scanning method totalling 50–90 seconds, was used for the Minolta scanner. The surface-to-surface distances of the facial images were compared, as well as the concordance of linear measurements. For linear measurements requiring identification of surface landmarks, the texture information was removed from the Vectra M3 scan in order to make it comparable to the non-textured laser scan. The mean surface-to-surface distance difference was 0.80 ± 0.41mm, the mean error for linear distances was 3.2 ± 1.3mm.

Planmeca ProMax 3D ProFace® (Planmeca USA, Inc.; Roselle, IL, USA) is a laser-based surface imaging system that is incorporated within a CBCT scanner. The 3D image can be taken independently of the CBCT scan and includes texture and colour information, the manufacturer claims a spatial accuracy of 0.03mm. In an investigation of anthropometric norms of a southern Spanish population, the system was validated by comparing 20 linear measurements from the 3D facial laser scans of 10 subjects to direct linear measurements. The subjects were not landmarked prior to scanning; the mean difference in linear measurements was reported to be 1.04mm, within the level of clinical acceptability (Menéndez López-Mateos *et al.*, 2019).

The reduced accuracy of laser scanners in vivo compared to other systems is likely because of motion error as a consequence of the increased scanning time, and the lack of texture information making landmark identification more difficult.

1.9 BELLUS3D

Bellus3D Face Camera Pro™ (Bellus Inc, California, USA) is an attachable camera system which uses tablet or smartphone software to capture, process and view 3D facial images. It is similar to active stereophotogrammetry as it projects a pattern of infrared dots over the subject's face and uses a camera to calculate the spatial location of each point. It requires the subject to turn their head 180-degree during capture and takes around 15 seconds in total to complete a facial scan.

1.9.1 In vitro validation

A comparative evaluation of the trueness of 3D facial scanning, of a mannequin head, using the Bellus3D Face Pro App on an iPhone X to a structured blue light 3D scanner

(ATOS Core, accuracy 3µm) scan has recently been reported (Gallardo *et al.,* 2023). The study used “best fit” of the facial scan meshes from each scanner and compared 50 landmark locations, grouped into 6 facial regions based on absolute distances closest point (Global trueness). For each image, the deviation value was reported as the absolute mean value of deviations of the points described by the 25 and 75% quantiles i.e., only the middle 50% of the points. All regions were accurate to within 1mm, the highest accuracy was found in the mentum and nasal areas and the least in the lateral areas of the face, the overall absolute mean value of deviations was 0.34 ± 0.14 mm.

The accuracy of Bellus3D Face Camera Pro has also been compared to both direct anthropometric measurements and 3dMD, using a mannequin head with 20 landmarks (Liu *et al.,* 2021). The mean absolute difference of eight linear distances between Bellus3D Face Camera Pro and direct anthropometric measurements was 0.61 ± 0.47mm, and between Bellus3D Face Camera Pro and 3dMD was 0.38 ± 0.37mm. The landmarks chosen were in the central portion of the face and not at the facial periphery; the outer limit of the eyebrow being the most lateral facial landmark. The study reported errors in the sub-nasal region because of shadowing. The same team repeated the study using the same methodology but using the Bellus3D ARC7, a system which uses multiple cameras to take a scan in 3 seconds and requires less patient movement (Pan *et al.,* 2022). The mean absolute difference of the eight linear distances between Bellus3D ARC7 and direct anthropometric measurements was 0.61 ± 0.42 mm, whilst between direct anthropometric measurements and 3dMD was 0.28 ± 0.14 mm.

1.9.2 In vivo validation

To assess the in vivo validity of Bellus3D Face Camera Pro, five linear distances of ten pre-landmarked scanned participants were compared to direct anthropometric measurements (Piedra-Cascón *et al.,* 2020). The acquisition time was measured at 15 seconds. Significant differences in inter-landmark measurements were reported in all subjects with an average distance of 0.91 ± 0.32 mm. None of the measurements recorded were from the facial periphery and as such the study only investigated the validity of Bellus3D Face Camera Pro in capturing the midline/para-midline regions as opposed to the whole face.

In order to try and standardise the Bellus3D scanning process, a novel scanning method was developed whereby the subjects head remained static, and the iPad Pro with Bellus3D app was attached to a slider track that moved around the patient (Raffone *et al.,* 2022). The study compared 23 linear distances from 10 scanned subjects, captured by rotating their heads and by sliding the iPad Pro around the head, to their direct anthropometric measurements. The results showed a mean absolute difference of 0.95 ± 0.25 mm for the conventional head rotating technique and 1.00 ± 0.29 mm for the slider technique. Even though the results were similar, less subject training was needed in the slider group.

A recent study has compared scans captured by Bellus3D Face App installed on an iPhone XS to those captured using 3dMD on 40 un-landmarked subjects (D'Ettorre *et al.*, 2022). Colour maps and surface to surface distance for 18 post-capture identified landmarks were compared. Repeatability and reproducibility of landmarking identification on the scanned images was very high. Colour mapping superimposition

showed an 80.01± 5.92% concordance between the systems to within 1mm. Thirteen of the 18 landmarks were within 1mm of each other. The study reported the most accuracy was associated with flat facial areas i.e. forehead chin and cheek, and the least in areas of curvature i.e. mouth lips and eyes. Wang et al. (2022) compared Bellus3D Dental Pro App and Bellus3D ARC7 to direct anthropometric measurements of 14 linear measurements, in 20 pre-landmarked subjects. Bellus3D Dental Pro App had the highest error (1.17 ± 0.80 mm), compared to the Bellus3D ARC7 system (0.76 ± 0.61 mm), the authors note that portability comes at the expense of slightly increased error. In a further study, based on 29 pre-landmarked subjects, comparing Bellus3D Face App to 3dMD, a mean surface to surface difference of 0.86 ± 0.31 mm was reported (Andrews et al., 2023). As well surface to surface measurement, point to point differences were also used, with 16 of the 18 landmarks found to be within 1 mm. Nasion was reported as the most accurate landmark, with gonion and tragion being the least accurate.

Thurzo et al. (2022) compared Bellus3D Dental Pro App installed on an iPhone X to sixty surface segmented CBCT scans (Thurzo et al., 2022). Colour maps were created showing differences >3mm, the most accurate area was found in convex areas of the midface, again with lateral and shadowed areas being less accurate. The highest error was found in the orbital area which was attributed to subjects usually having their eyes open for the Bellus3D scan and closed for the CBCT scan (Thurzo et al., 2022). In a similar study comparing Bellus3D ARC1 to facial CBCT scans, all measurements and angles were within 1.5mm or 1.5° of each other apart from two vertical measurements, Subnasale-Pogonion and Sellion-Subnasale, which were attributed to inaccuracy of sub-nasale (Aljawad *et al.,* 2022).

1.10 REPRODUCIBILITY OF SMILE EXPRESSION

To date all the studies using Bellus3D have recorded the individual at rest or neutral facial expression. Many of the other established systems have been used to investigate the reproducibility of various facial expressions (Johnston *et al.,* 2003; Sawyer *et al.,* 2009)..

Reproducibility of facial expression is essential when assessing the effect of an intervention; any measurable changes need to be a result of the intervention and not because the facial expression unreproducible. Since the face is a dynamic structure, rest position, requiring minimum muscular control has been shown to be the most reproducible facial expression (Johnston *et al.,* 2003; Sawyer *et al.,* 2009). Interestingly, most facial expressions are reproducible in the short term, with minimal differences found between images taken 15 minutes apart (Sawyer, et al., 2009). Reproducibility was found to reduce with increasing time between scans (2 - 4 weeks interval) however these differences were small (<1.0mm) and unlikely to be clinically significant (Johnston *et al.,* 2003, Sawyer *et al.,* 2009; Tanikawa and Takada, 2018). Smiling is one of many non-verbal facial expressions that are important for aesthetic and social reasons. In terms of smile reproducibility, both maximum smile and social smile have been investigated (Johnston e*t al.,* 2003). Maximum smile was found to be more reproducible and it was suggested that this was because maximum smile allows for less variability of movement since the muscle and fascia are at the extreme end of stimulation (Johnston e*t al.,* 2003; Tanikawa and Takada, 2018; Khambay *et al.,* 2019). Nevertheless studies of reproducibility of social smiles in the short and long term showed clinically acceptable reproducibility to within 1.5mm (Dindaroğlu *et al.*, 2016; Dobreva *et al,* 2022).

1.10.1 Applications of facial smile scans

3D facial smile scans are useful in medicine to identify the numerous facial movements that occur during smile. The application of this information could be for aesthetic purposes, e.g., the identification of key muscle groups as targets for Botox® in an asymmetric or gummy smile, or as a guide for smile re-animation in patients who have suffered facial palsy (Sun *et al.,* 2022). As with non-smiling scans comparisons can be made pre- and post-treatment to evaluate the effects of the intervention such as re-innervation surgery or facelift surgery (Li *et al.,* 2015; Gibelli *et al.,* 2020). Individuals often seek treatment to improve their smiles (Millsopp *et al.,* 2006). Following the introduction of extra-oral and intra-oral scanning, reverse engineering, and CAD/CAM technology “smile design technology” is commonly utilised in restorative treatment planning. The various images are used to simulate dental and gingival changes needed to achieve ideal aesthetics. In this approach the intraoral scan can be combined with a smiling extraoral scan to produce a digital patient. Treatment can be planned relative to the face, providing improvements in diagnosis, treatment planning, communication with the technician and informed consent (Finelle, 2017; Jreige *et al.,* 2022). As well as restorative dentistry, three dimensional smiling images can also be used in orthodontics to determine treatment goals, for example it is useful to know lip position during smile in order to plan the position of the upper incisors and treatment can be simulated to evaluate the effect of dental movements on the soft tissues (Finelle, 2017; Demir and Baysal, 2020; Jreige *et al.,* 2022). Treatment outcomes can be evaluated by comparing pre- and post-treatment scans (Dindaroğlu *et al.,* 2016).

1.11 SUMMARY

Thus, the evidence shows that structured light-based systems performed better than laser systems when compared to direct measurements or stereophotogrammetry. Overall, the results demonstrate that the faster the system is able to capture data the more accurate it is, and that more economical and portable systems with a longer scanning time come at the expense of this accuracy, the information is summarised in Tables 1.1 to Table 1.4.

Ideal Feature	Laser	Structured Light	Stereophotogrammetry
Portable	Yes	Yes	No
Economical	Yes	Yes	No
Biocompatible	Risk of eye damage	Yes	Yes
Surface texture & colour	No	Yes	Yes
Scanning time	Up to 30s	Up to 30s	<1s
Reproducible	Yes	Yes	Yes

Table 1.1 Summary comparison of 3D scanning systems

Table 1.2 Summary table of studies

Study	Experimental system	N	Pre-marked face	Control	Method of analysis	Results
Ma *et al.,* 2009	Structured Light	3 plaster models	Yes	CMM	Mean deviation from CMM central point for 19 landmarks	0.93 ± 0.36mm
Artopoulos *et al.,* 2014	Projection Moirè Topography	22 mid face plaster models	No	Segmented surface CT	Iterative closest point matching algorithm. colour-coded maps of differences	95.1% within 1mm
Winder *et al.,* 2008	Stereophotogrammetry (Di3D)	Mannequin head	Yes	Direct Anthropometry	20 Linear distances between landmarks	0.62mm
Lubbers *et al.,* 2010	Stereophotogrammetry (3dMD)	Mannequin head	Yes	Direct Anthropometry	201 linear distances between 41 landmarks	0.01 ± 0.55mm
Camison *et al.,* 2018	Portable Stereophotogrammetry (Vectra H1)	Mannequin head	Yes	Stereophotogrammetry (3dMDface)	Shape-based Levenberg–Marquardt curve-fitting algorithm. Surface to surface RMS	0.144 mm
Kusnoto *et al.,* 2002	Laser (Minolta Vivid700)	1 plaster model	Yes	Direct Anthropometry	21 linear measurements	1.9mm ± 0.8mm

Study	Experimental system	N	Facial Expression	Pre-marked face	Control	Method of analysis	Results
Dindaroglu *et al.,* 2016	Stereophotogrammetry (3dMDflex)	80	Not known	No	Direct Anthropometry	10 Linear distances between landmarks	All within 0.25mm
Wong *et al.,* 2008	Stereophotogrammetry (3dMDface)	20	Not known	No	Direct Anthropometry	18 Linear distances between landmarks	17 of 18 linear distances within 1.2mm
Camison *et al.,* 2018	Portable Stereophotogrammetry (Vectra H1)	23	Neutral	Yes	Stereo photogrammetry (3dMDface)	136 linear distances between landmarks	0.84 mm
						Shape-based Levenberg–Marquardt curve-fitting algorithm. Surface to surface RMS	0.43 mm
Kovacs *et al.,* 2006	Laser (Minolta Vivid 910)	5	Not known	Yes	Direct Anthropometry	345 linear distances between landmarks	1.32 ± 5.67mm
Menéndez López-Mateos *et al.,* 2019	Laser (Planmeca ProMax 3D ProFace)	10	Neutral	No	Direct Anthropometry	20 linear distances between landmarks	Mean difference 1.04mm
Gibelli *et al.,* 2018	Laser (Minolta Vivid 910)	15	Neutral	No	Stereo photogrammetry (Vectra M3)	RMS point-to-point distance	0.80 ± 0.41mm
						14 linear distances	3.2 ± 1.3mm

Table 1.3 Summary comparison of in vitro Bellus3D studies

Study	Experimental system	Facial Expression	Pre-marked face	Control	Method of analysis	Results
Gallardo *et al.,* 2021	Bellus 3D Face App on iPhone X	N/A	No	ATOS Core structured blue light 3D scanner	Best fit mesh based on absolute distances closest point (Global trueness). A mean of 30 to 50 points was defined as acceptable. For each point, the deviation value was determined as the absolute mean value of deviations, which lies within an interval comprising 50% of the measuring points, described by the 25 and 75% quantiles	0.34 ± 0.14mm
					3D measurement of 50 landmarks based on absolute distances	<1.0mm
Liu *et al.,* 2021	3dMDface system	N/A	Yes	Direct anthropometry	Linear distances between landmarks	0.38 ± 0.37mm
	Bellus3D Face Camera Pro					0.61 ± 0.47mm
Pan *et al.,* 2022	3dMDface system	N/A	Yes	Direct anthropometry	Linear distances between landmarks	0.28 ± 0.14mm
	Bellus3D ARC-7					0.61 ± 0.42mm

Table 1.4 Summary comparison of in vivo Bellus3D studies

Study	Experimental system	N	Facial Expression	Pre-marked face	Control	Method of analysis	Results
Piedra-Cascón *et al.*, 2020	Bellus3D Face Camera Pro	10	"Avoid facial expression"	Yes	Direct anthropometry	5 Linear distances between landmarks	0.91 ± 0.32 mm
Wang *et al.*, 2021	Bellus3D Face App	20	Rest	Yes	Direct anthropometry	14 Linear distances between landmarks	1.17 ± 0.8 mm
	Bellus3D ARC-1	20	Rest	Yes	Direct anthropometry	14 Linear distances between landmarks	0.76 ± 0.61 mm
D'Ettorre *et al.*, 2022	Bellus3D Face App	40	Rest	No	3dMDtrio	Best-fit alignment Surface to surface distance	80.01 ± 5.92% within 1 mm
		40	Rest	No		Best-fit alignment Point to point distance (x, y & z)	13 of 18 landmarks within 1 mm

Table 1.4 Summary comparison of in vivo Bellus3D studies (continued)

Study	Experimental system	N	Facial Expression	Pre-marked face	Control	Method of analysis	Results
Raffone *et al.,* 2022	Bellus3D Face App	10	Rest	Yes	Direct anthropometry	23 Linear distances between landmarks	0.95 ± 0.25 mm
Thurzo *et al.,* 2022	Bellus3D Face App	60	Rest	No	Segmented facial surface CBCT	Best fit and Measurement of 21 colour map regions	Significant differences in some facial regions > 3 mm
Aljawad *et al.,* 2022	Bellus3D ARC-1	25	Not known	No	Segmented facial surface CBCT	Best-fit alignment 23 Linear distances between landmarks	21 of 23 inter-landmark distance within 1.5 mm
Andrews *et al.,* 2023	Bellus3D Face App	29	Rest	Yes	3dMDface	Best-fit alignment Surface to surface distance	0.86 ± 0.31 mm
		29	Rest	Yes		Best-fit alignment Point to point distance	16 of 18 landmarks within 1.0 mm

CHAPTER 2

AIMS & NULL HYPOTHESIS

2.1 AIMS

2.1.1 In vitro

The aims of the in vitro study were to determine the validity and accuracy of two Bellus3D devices - Bellus3D Face Camera Pro (Android device) and Bellus3D and iPhone 12 (Apple device), and two commercial 3D facial imaging systems - 3dMD and Di4D SNAP.

Primary outcome measure

1. The mean difference in Euclidean distance between 35 pre-marked facial landmarks captured using the Bellus3D devices and the commercial devices.

2.1.2 In vivo

The aims of the in vivo study were to determine the validity and accuracy of Bellus3D Face Camera Pro (Android device) compared to an established clinically validated stereophotogrammetry based system, Di4D SNAP whilst capturing the face at rest and at maximum smile.

Primary outcome measures include:

1. The mean difference in Euclidean distance between 21 pre-marked facial landmarks captured using Bellus3D Face Camera Pro (Android device) and Di4D SNAP.

Secondary outcome measures include:

1. The mean differences in x, y and z co-ordinates between 21 pre-marked facial landmarks captured using Bellus3D Face Camera Pro (Android device) and Di4D SNAP.

2.2 NULL HYPOTHESIS

2.1 In vitro

There is no statistically significant difference ($p<0.05$) in the position (based on the Euclidean distance) of 35 facial landmarks, captured using the Bellus3D devices and the commercial systems.

2.2 In vivo

The mean differences in Euclidean distance of 21 facial landmarks, at rest and at maximum smile, captured using Bellus3D Face Camera Pro and Di4D SNAP, were not statistically significantly different to the clinically significant mean distance of 2.0mm.

CHAPTER 3

MATERIALS AND METHODS

3.1 IN VITRO VALIDATION OF BELLUS3D SYSTEMS, 3dMD AND DI4D SNAP

3.1.1 Gold standard reference data

A plastic mannequin head was pre-marked with 35 facial landmarks using a fine black ink pen (Lumocolor, Staedtler, Germany), Figure 3.1. The plastic mannequin head was digitised three times over 2 days, by a highly trained operator (RH), using a Mitutoyo CMM EURO-C-A544 coordinate measuring machine (CMM) (Mitutoyo Corporation, Kanagawa, Japan) at the Department of Mechanical Engineering, University of Birmingham, Figure 3.2. The CMM comprised of a stylus or touch probe, which was used to determine the three-dimensional coordinates of each of the 35 landmarks. The coordinate data were saved in Excel (Microsoft Corporation, USA). The mean of the three sets of coordinate data was used as the "gold standard", and as a reference to evaluate the accuracy of the four three-dimensional imaging systems i.e., Bellus3D Face Camera Pro (Andoid), Bellus3D Application (app) and iPhone 12, 3dMD and Di4D SNAP.

3.1.2 Image capture using Bellus3D and Bellus3D Face Camera Pro (Android device)

The pre-landmarked plastic mannequin head was placed on a turntable, which allowed 360^{o} rotation of the head, Figure 3.3. A Huawei MediaPad T3 Tablet (Huawei UK, Berkshire, UK) and Bellus3D Face Camera Pro (#1300 Campbell, CA 95008), with Bellus3D app (Face Camera Pro for Android (Service) Release: 2.1.1) installed, were placed directly in front of the plastic head. Prior to imaging the mannequin head the Bellus3D app was calibrated according to the developer's instructions. The Bellus3D system was secured to a tablet holder, which allowed multi-directional movement of the tablet and camera, Figure 3.4. The position of the mannequin head was determined

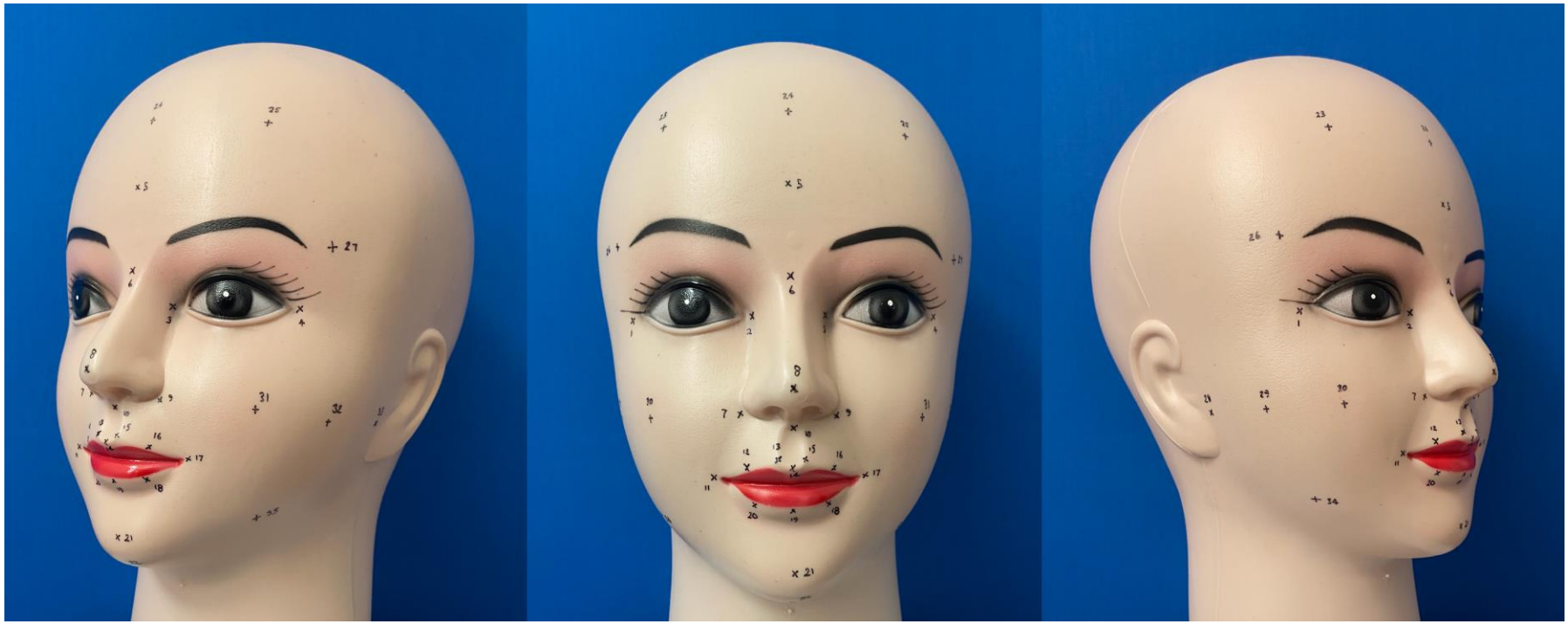

Figure 3.1 Plastic mannequin head was pre-marked with 35 facial landmarks.

Figure 3.2 Mitutoyo CMM EURO-C-A544 coordinate measuring machine (CMM) (Mitutoyo Corporation, Kanagawa, Japan).

Figure 3.3 Pre-landmarked plastic mannequin head on a turntable, which allowed 360º rotation of the head.

Figure 3.4 Bellus3D system secured to a tablet holder, allowing multi-directional movement of the tablet and camera.

by the Bellus3D app, which instructed the user to place the face of the mannequin within an oval boundary. Once the face was correctly positioned, with the oval boundary turning green, the instructions given by the Bellus3D app were followed, Figure 3.5. The face was rotated to the left, back to the middle and then to the right over a specific time period indicated by a countdown timer on the app. The mannequin head was rotated as if it were a human head and scanned twice using the High Definition (HD) mode and each image saved in Wavefront .OBJ format. The OBJ format is a universal 3D model format widely supported by 3D image editing applications. The format is simple and text-based and produces 3D images with photo-realistic texture.

3.1.3 Image capture using Bellus3D app and iPhone 12 (Apple device)

The pre-landmarked plastic mannequin head was placed on a turntable. An Apple iPhone 12 (Apple Distribution International Ltd, Cork, Republic of Ireland) with Bellus3D app (version 1.8.9) installed was secured to the tablet holder and the face of the mannequin was captured following the app instructions as described in Section 3.1.2. The mannequin head was rotated as if it were a human head and scanned twice using the High Definition (HD) mode and each image saved in Wavefront .OBJ format.

3.1.4 Image capture using 3dMD

The mannequin head was imaged using 3dMD. The 3dMDface system (3dMD Inc., Atlanta, GA, USA) comprised of two vertical banks of six medical-grade cameras with industrial-grade flash systems, Figure 3.6. The cameras were fixed at different angles to simultaneously capture images of the face from ear to ear. The capture speed was approximately 1.5 milliseconds.

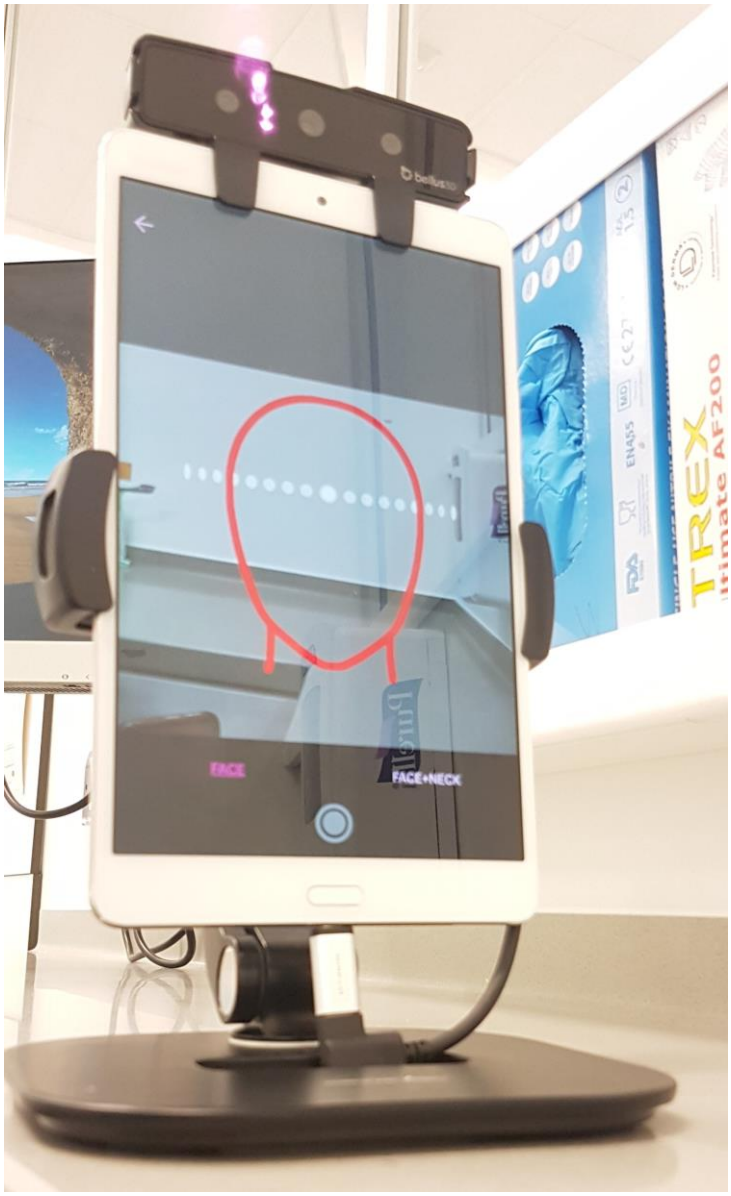

Figure 3.5 Bellus3D showing position of face for scanning, turns green when correct.

Figure 3.6 3dMDface system (3dMD Inc., Atlanta, GA, USA).

3.1.5 Image capture using Di4D SNAP

The mannequin head was imaged using Di4D SNAP (Dimensional Imaging Ltd, Hillington, Glasgow, UK). This was as 6 camera based 3D passive stereophotogrammetry system developed to capture high resolution 3D facial images, Figure 3.7. The system comprised of 2 Canon cameras (XX) arranged in three vertical banks connected to a personal computer (PC) and two commercial white-light studio flash units (Esprit Digital DX1000, Bowens, Essex, UK). It took 1 ms to capture the face with the Di4D SNAP system.

3.1.5.1 System calibration

Prior to image capture both 3dMD and Di4D systems required calibration. The purpose of the calibration was to determine the intrinsic and extrinsic camera properties and relative location of each camera pair to one another. Calibration consisted of imaging a manufacture provided calibration target at different orientations. The calibration target consisted of a series of dots at a known distance separation. The calibration software used these dots and compared the changes in distance between the centers of the dots to determine the dimension of depth, based on the principle of triangulation. This calibration information was saved as a calibration file which needed be attached to the facial image, in a later stage, to allow re-construction of the 3D facial image. The systems were calibrated at the beginning of each facial capture session.

3.1.5.2 Image capture

The mannequin head was secured to a tripod (Manfrotto, Italy) and placed at a distance from the camera system based on the manufactures instructions. The face of the mannequin head was imaged and saved in Wavefront .OBJ format. One week later

Figure 3.7 Di4D SNAP (Dimensional imaging)

the entire procedure was repeated, so that two three-dimensional models were produced for the mannequin head, one from each session.

3.1.5.3 Digitisation of landmarks

The 3D images (.OBJ) generated using each of the Bellus3D systems were loaded into DiView (Dimensional Imaging) which allowed the 3D image to be rotated / zoomed and viewed in simultaneously in three separate windows on the single PC monitor, Figure 3.8. This allowed accurate identification and landmark placement in three planes of space. The landmarks of each three-dimensional model were digitised by one observer (KT) on two separate occasions. DiView software recorded the x, y, and z coordinates of each of the 35 landmarked and exported them to EXCEL. The same procedure was repeated for the 3D facial images of the mannequin head captured by Di4D SNAP and 3dMD.

3.2 IN VIVO CLINICAL VALIDATION OF BELLUS3D FACE CAMERA PRO AND DI4D SNAP

A formal sample size calculation was undertaken and determined that a minimum sample of 30 volunteers was required, at a significance level of 0.05 and power of 80%, to detect a 1mm difference in landmark position between Di4D SNAP system and Bellus3D Face Camera Pro. Previous studies have suggested that a difference of 2.0 mm was deemed to be clinically significant and reported a standard deviation of ± 1.0 mm in differences in landmarks.

Figure 3.8 DiView (Dimensional Imaging) showing 3D simultaneously viewed on three separate windows on the single PC monitor.

3.3 ETHICAL APPROVAL

Ethical approval to conduct the study using volunteers was sought and granted by the University of Birmingham Ethical review committee (ERN_19-0165).

3.4 STUDY PARTICIPANTS

30 volunteers from staff and students at the Birmingham Dental Hospital and School were invited to take part in the study from July 2020 to August 2020. Adults, who fulfilled the inclusion criteria, were given a volunteer information sheet (Appendix I) and invited to voluntarily participate in the study. They were given at least 1 week to consider the information and whether they wished to participate to ensure their consent was given voluntarily. They could waive the waiting period if they chose to. Once the volunteer had decided to participate, they were asked to complete a consent form (Appendix II) which detailed that their data would be anonymised and that they may withdraw their consent.

3.4.1 Inclusion criteria

The inclusion criteria for the study were as follows, patients who

- Were between 18-50 years.
- Were willing to participate and provide written consent.
- Males had no facial hair.
- Individuals with facial covering that did not prevent full facial soft tissue exposure.
- Were English speaking.

3.4.2 Exclusion criteria

The exclusion criteria were as follows,

- A craniofacial syndrome.
- Had facial hair.
- Were non-English speaking.
- Individuals with facial covering that prevented full facial soft tissue exposure.
- Patients not willing to participate in the study.

3.5 IMAGING OF VOLUNTEERS

3.5.1 Pre-imaging preparation

Prior to image capture, 21 standard landmarks were placed on each volunteer's face using a Khol eyeliner pencil (Max Factor Cosmetics Limited, Rhondda Cynon Taf, U.K.), Table 3.1. Following this each volunteer was trained by the researcher (KT) to achieve rest position and perform a maximum lips apart smile with their teeth in maximum intercuspation, Figure 3.9. The facial expressions were demonstrated until the volunteers were comfortable performing the rest and maximum smiles facial expression. Rest position was achieved by asking the subject to say 'Mississippi', and then told to swallow once and say 'N' (Zachrisson, 1998). Maximal smile was achieved by asking subjects to bite their teeth tightly together and smile maximally (Johnston *et al.,* 2003).

3.5.2 Bellus3D

Each volunteer was shown and instructed how to use the Bellus3D capture system. This was important as they needed turn their head the full 180° from ear to ear at the appropriate speed, following the verbal instructions given by the app. This was

Table 3.1 21 standard landmarks placed on each volunteer's face prior to imaging

Landmark	Definition
1	Right forehead
2	Mid forehead
3	Left forehead
4	Right exocanthus
5	Glabella
6	Left exocanthus
7	Right cheek (midpoint between LM4 and 13)
8	Nasal tip
9	Left cheek (midpoint between LM6 and 17)
10	Right alar base
11	Left alar base
12	Right gonion
13	Right cheilion
14	Right philtrum
15	Mid philtrum
16	Left philtrum
17	Left cheilion
18	Left gonion
19	Mid lower lip
20	Pogonion
21	Menton

Figure 3.9 Volunteer in rest position and maximum lips apart smile with their teeth in maximum intercuspation captured using Bellus3D and Di4D SNAP.

rehearsed several times until each volunteer was comfortable performing the instructions. They were asked to remove any glasses to prevent reflections. Loose hair strands over the face had the potential to distort the facial image; therefore, surgical head caps were provided, if required, to hold any hair away from the forehead and surrounding area. Each volunteer was asked to sit on a chair facing the Bellus3D system which was secured in the tablet holder. Additional 26cm ring LED flashes (AIXPI, Guangming New District, Shenzhen, China) were positioned above and below the volunteer's face for supplemental lighting. The Bellus3D app, instructed the user to position their face within the red oval boundary, which then turned green if correctly positioned. Once correctly positioned the Bellus3D app instructed the volunteer to rotate their face to the left, back to the middle and then to the right over a specific time period indicated by a countdown timer on the app. The app indicated to the user when the scan was complete. Each volunteer was captured in natural head position, at rest and at maximal smile.

3.5.3 Di4D SNAP system

Following Bellus3D image capture, volunteers were seated in front of a blue screen and the Di4D SNAP camera system. They were asked to remove any glasses to prevent reflections. Loose hair strands over the face had the potential to distort the facial image; therefore, surgical head caps were provided, if required, to hold any hair away from the forehead and surrounding area. The position of the volunteer was adjusted until they were correctly positioned relative to the camera system using the cross-hair locators seen on the capture software. As before, each volunteer was then captured in rest position and at maximal smile; again, both images were saved in .OBJ format and landmarked as previously described (**3.1.5.3**).

3.6 PRELIMINARY INVESTIGATION TO DETERMINE REST POSITION STABILITY

The reproducibility of rest position was assessed by taking two images, 10 minutes apart of 10 random volunteers using the Di4D system. Both images were saved in .OBJ format and landmarked as previously described (**3.1.5.3**).

3.7 LANDMARKING IDENTIFICATION ERROR

The reproducibility of landmark identification was assessed using ten randomly selected 3D images. Each image was landmarked on two occasions, at least 2 weeks apart, and the differences in landmark position in the x, y and z direction, between the first and second digitisation were analysed. Systematic error was assessed by using a Students paired t-tests and random error assessed by coefficients of reliability (Houston, 1983).

3.8 ANALYSIS

3.8.1 In vitro validation of Bellus3D and Di4D SNAP

Following digitisation of each facial image of the mannequin plastic head, a 3D landmark configuration of 35 landmarks was produced. Code was written in MATLAB to read in the x, y and z co-ordinates of each of the 35 landmarks, producing a 3D landmark configuration, Figure 3.11. The landmarks generated by the CMM were aligned using partial Procrustes superimposition, with no scaling or reflection, to the 3D landmark configuration of the 35 landmarks produced following digitisation of the mannequin plastic head captured using the Bellus3D and Bellus3D Face Camera Pro (Android device). Procrustes superimposed, translated and rotated the two 3D landmark configurations to achieve the “best-fit” minimising the distance between the

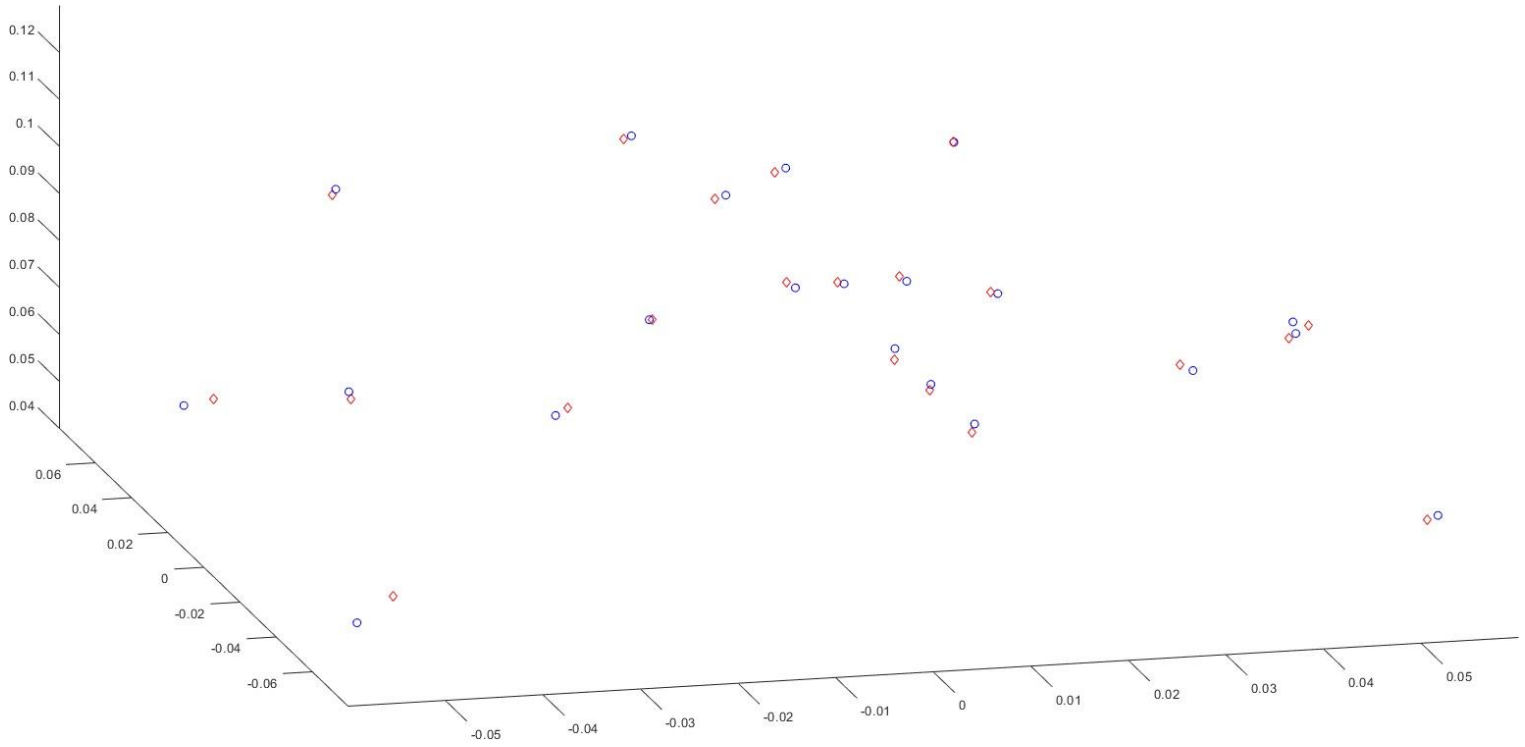

Figure 3.10 3D landmark configurations.

landmark configurations. If the two landmark configurations were identical, then the distance between each corresponding landmark pair would be zero. The larger the difference in distance between landmark pairs, the greater the error or difference between the landmark pairs and therefore configurations. The distance between the landmark pairs was measured in several different ways; as a Euclidian distance, differences in each of the 3 directions means, as a signed difference and as an absolute difference. The sign, either +ve or –ve, was indicative of the direction of error whilst the absolute distance was irrespective of direction. The difference between each of the 35 landmarks pairs, between the CMM and the five Di4D SNAP images, were saved in EXCEL for further analysis. The 3D landmark configurations, 5 for each, using Bellus3D and iPhone 12, 3dMD, and Di4D SNAP were in turn compared to the gold standard CMM configuration. For each pair of landmarks, the measurements highlighted above were determined.

3.8.2 Landmarking identification error

Systematic error of landmark placement was assessed using a Students paired *t*-tests and random error was assessed by coefficients of reliability (Houston, 1983).

3.8.3 In vivo clinical validation of Bellus3D and Di4D SNAP (clinical gold standard)

Two 3D landmark configuration of 21 landmarks were produced following digitisation of each volunteer's facial image at rest using Bellus3D and Bellus3D Face Camera Pro (Android device) and Di4D SNAP. The two 3D landmark configurations were aligned using partial Procrustes superimposition, with no scaling or reflection as above. The difference between each of the 21 landmarks pairs, were saved in EXCEL for further

analysis. This was repeated using the two 3D landmark configuration of 21 landmarks produced following digitisation of each volunteer's facial image at maximal smile using Bellus3D and Bellus3D Face Camera Pro (Android device) and Di4D SNAP.

CHAPTER 4

RESULTS

4.1 DEMOGRAPHICS

In total 30 individuals were recruited for this study, 12 male and 18 females. The age range was from 22 to 42.

4.2 IN VITRO VALIDATION OF IMAGING SYSTEMS

The mean differences in Euclidean distances between the “gold standard” co-ordinate measuring machine (CMM) 3D configuration, based on 35 landmarks (LM), and each of the 3D configuration produced by the four imaging systems is shown in Table 4.1

4.2.1 3dMD versus Co-ordinate Measuring Machine (CMM)

For 3dMD the mean differences in Euclidean distances ranged from 0.2mm at right philtrum (LM13) to 1.5mm for right gonion (LM34). Thirty of the 35 landmarks showed a mean difference of 1.0mm or less. The mean difference in Euclidean distances between the CMM and 3dMD across the 35 landmarks was 0.7 ± 0.3mm.

4.2.2 Di4D SNAP versus Co-ordinate Measuring Machine (CMM)

For Di4D SNAP the mean differences in Euclidean distances ranged from 0.2mm for glabella, right upper lip, right and mid philtrum and left upper lip (LM5, 12, 13, 14 and 16) to 1.4mm for right zygoma (LM29). Thirty-one of the 35 landmarks showed a mean difference of 1.0mm or less. The mean difference in Euclidean distances between the CMM and Di4D SNAP for all the landmarks was 0.6 ± 0.3mm.

Following a Kolmogorov–Smirnov test to confirm data normality, a two-sample Students t-test confirmed the mean difference in Euclidean distance between 3dMD and Di4D SNAP (0.1 ± 0.04mm) was not statistically or clinically significant (p = 0.244,

Table 4.1 Mean (±SD) differences in Euclidean distances between the "gold standard" co-ordinate measuring machine (CMM) 3D configuration and each of the four imaging systems.

Landmark No	Landmark Description	Mean difference 3dMD (mm)	Mean difference Di4D SNAP (mm)	Mean difference Face Camera Pro (mm)	Mean difference iPhone + Bellus3D app (mm)
1	R outer canthus	0.8	0.7	1.7	1.1
2	R inner canthus	0.4	0.3	0.8	1.2
3	L outer canthus	0.5	0.4	1.5	2.0
4	L inner canthus	0.5	0.8	1.4	0.9
5	Glabella	0.7	0.2	0.9	1.0
6	Nasion	0.4	0.4	0.4	0.8
7	R alar base	0.8	0.7	0.9	1.1
8	Nasal tip	0.8	0.9	0.8	1.1
9	L alar base	0.8	0.5	1.9	1.6
10	Sub nasale	0.6	0.3	1.0	0.9
11	R cheilion	0.6	0.6	1.1	0.9
12	R upper lip	0.3	0.2	0.5	0.6
13	R philtrum	0.2	0.2	0.6	0.9
14	Mid philtrum	0.4	0.2	0.6	0.9
15	L philtrum	0.4	0.3	0.6	0.7
16	L upper lip	0.3	0.2	0.9	0.7
17	L cheilion	1.3	1.0	1.9	1.6
18	Left lower lip	0.4	0.5	0.7	0.9
19	Mid lower lip	0.6	0.6	1.0	1.1
20	Right lower lip	1.0	0.7	0.7	1.3
21	Gnathion	0.5	0.7	1.3	1.0
22	Menton	0.7	0.6	9.6	8.5
23	R forehead	0.4	0.4	1.6	1.9
24	Mid forehead	0.4	0.3	1.6	1.9
25	L forehead	0.9	0.4	1.6	2.2
26	R eyebrow	0.5	0.4	1.5	0.9
27	L eyebrow	0.8	0.7	1.2	1.5
28	R EAM	0.5	0.7	2.8	1.2
29	R zygoma	1.3	1.4	0.9	1.3
30	R cheek	0.6	0.4	0.4	0.9
31	L Cheek	0.5	0.3	0.9	1.0
32	L zygoma	1.4	1.2	1.3	2.6
33	L EAM	0.7	0.4	2.8	2.0
34	R gonion	1.5	1.3	1.4	1.8
35	L gonion	1.1	1.1	1.8	4.8
	Mean	**0.7**	**0.6**	**1.4**	**1.6**
	SD	**0.3**	**0.3**	**1.5**	**1.4**

95% CI for the difference -0.1mm to 0.2mm). The distribution of the landmarks with difference in Euclidean distance greater than 1.1mm was similar in both systems and involved peripheral landmarks, Figure 4.1.

4.2.3 Bellus3D app and Bellus3D Face Camera Pro (Android device) versus Co-ordinate Measuring Machine (CMM)

For Bellus3D Face Camera Pro the mean differences in Euclidean distances ranged from 0.4mm for nasion and right cheek (LM6 and 30) up to 9.6mm for menton (LM22). Seventeen of the 35 landmarks showed a mean difference of 1.0mm or less, 17 landmarks from 1.1mm to 3.0mm and one landmark above 3.1mm. The mean difference in Euclidean distances between the CMM and Bellus3D Face Camera Pro was 1.4 ± 1.5mm.

4.2.4 Bellus3D app and iPhone 12 (Apple device) versus Co-ordinate Measuring Machine (CMM)

For the iPhone 12 and Bellus3D app, the mean differences in Euclidean distances between the 35 landmarks ranged from 0.6mm for right upper lip (LM12) up to 8.5mm for menton (LM22). Fifteen of the 35 landmarks showed a mean difference of 1.0mm or less, 18 landmarks from 1.1mm to 3.0mm and 2 landmarks above 3.1mm.

The mean difference in Euclidean distances between the CMM and iPhone and Bellus3D app was 1.6 ± 1.4mm. Following a Kolmogorov–Smirnov test to confirm data normality, a two-sample Students *t*-test confirmed the mean difference in Euclidean distance between Bellus3D Face Camera Pro and the iPhone 12 and Bellus3D app combination (-0.1 ± 0.7mm) was not statistically or clinically significant (p = 0.735, 95%

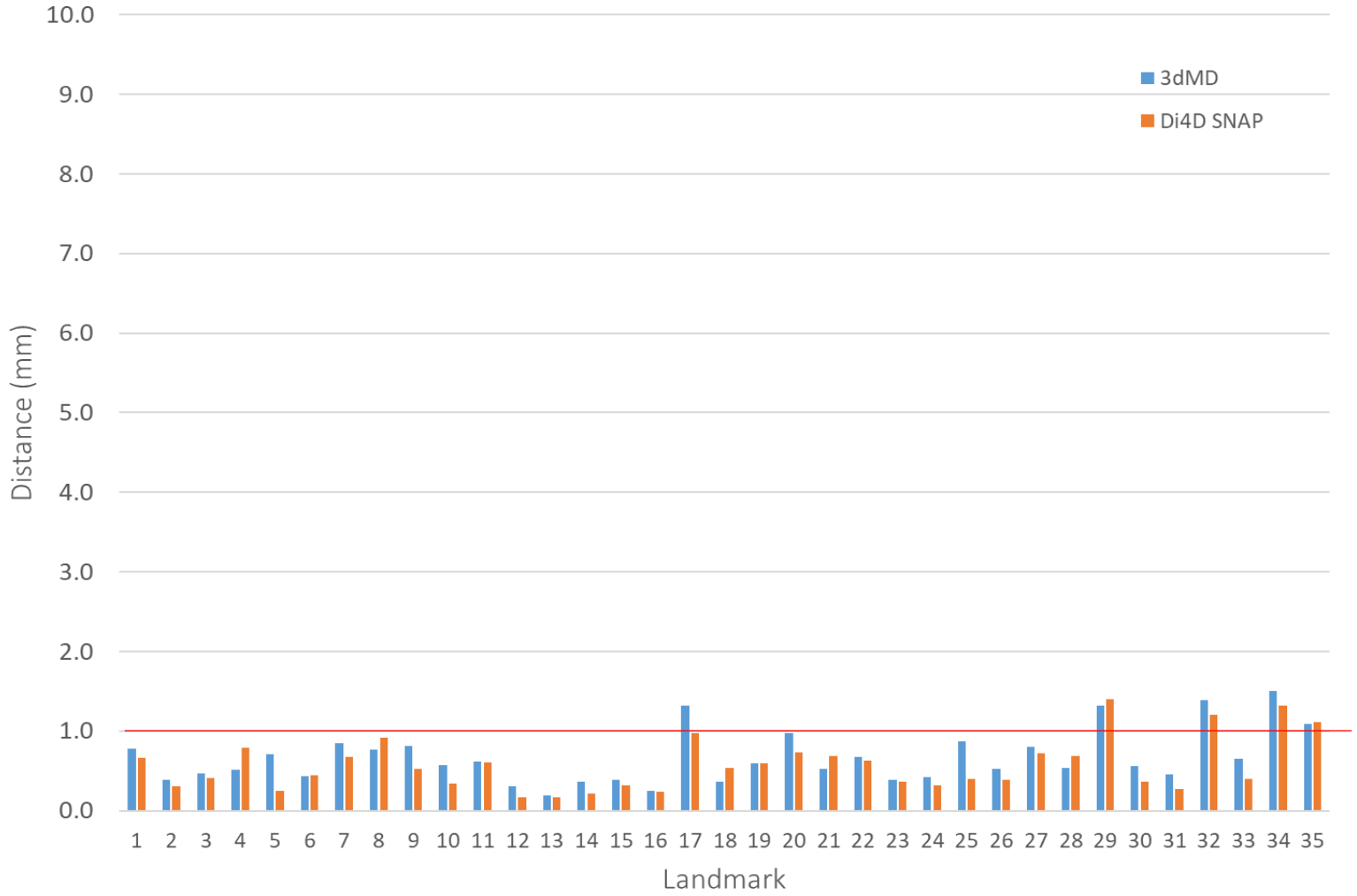

Figure 4.1 Mean Euclidean distance (mm) between the co-ordinate measuring machine (CMM) landmark and the 3dMD and Di4D SNAP landmark for the mannequin head. Red line at 1.0mm difference.

CI for the difference -0.8mm to 0.6mm), Figure 4.2 The distribution of the landmarks with difference in Euclidean distance greater than 1.1mm was similar in both systems and involved many of the peripheral landmarks.

4.2.5 Commercial systems versus Bellus3D devices

Table 4.2 shows the mean differences in Euclidean distances between the two commercial systems (combined mean 3dMD and Di4D SNAP) and the Bellus3D devices (combined mean Bellus3D Face Camera Pro and iPhone 12 and Bellus3D app), Figure 4.3. Following a Kolmogorov–Smirnov test to confirm data normality, a two-sample Students *t*-test showed the mean difference in Euclidean distance (0.9 ± 1.4mm) between the commercial systems and the Bellus3D devices was statistically significant (p = 0.001) with a 95% confidence interval for the difference of -1.4mm to -0.4mm).

4.3 IN VIVO CLINICAL VALIDATION OF BELLUS3D FACE CAMERA PRO AND DI4D SNAP

4.3.1 Landmarking identification error

Table 4.3 shows the landmark error study based on the mean (±SD) absolute distances in the x, y and z-direction. No systematic errors were observed, with all p-values > 0.05 following the Students paired *t*-test. All coefficients of reliability were above 90%. Based on the mean of the absolute distances, landmarks were digitised to within 0.23 ± 0.07 mm in the x-direction, 0.24 ± 0.06 mm in the y-direction and 0.15 ± 0.09 mm in the z-direction.

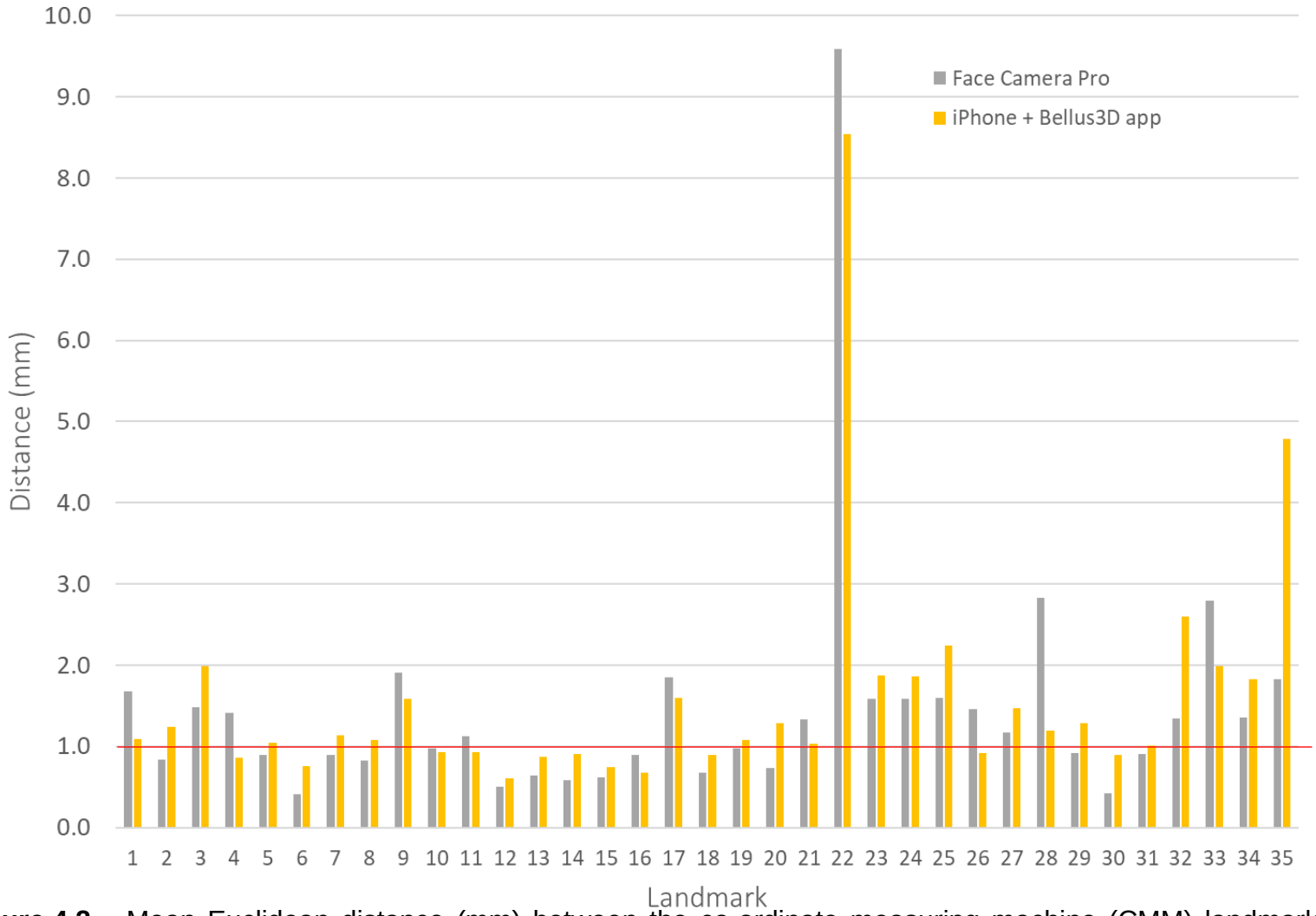

Figure 4.2 Mean Euclidean distance (mm) between the co-ordinate measuring machine (CMM) landmark and the Bellus3D Face Camera Pro and iPhone + Bellus3D app. Red line at 1.0mm difference.

Table 4.2 Mean (±SD) differences in Euclidean distances between the two commercial systems (combined mean 3dMD and Di4D SNAP) and the Bellus3D devices (combined mean Bellus3D Face Camera Pro and iPhone and Bellus3D app)

Landmarks	Commercial systems (3dMD and Di4D SNAP)	Bellus3D devices (Face Camera Pro) and iPhone app	Difference
1	0.7	1.4	0.7
2	0.3	1.0	0.7
3	0.4	1.7	1.3
4	0.6	1.1	0.5
5	0.5	1.0	0.5
6	0.4	0.6	0.1
7	0.8	1.0	0.3
8	0.8	1.0	0.1
9	0.7	1.7	1.1
10	0.5	0.9	0.5
11	0.6	1.0	0.4
12	0.2	0.6	0.3
13	0.2	0.8	0.6
14	0.3	0.7	0.5
15	0.4	0.7	0.3
16	0.2	0.8	0.5
17	1.1	1.7	0.6
18	0.5	0.8	0.3
19	0.6	1.0	0.4
20	0.9	1.0	0.2
21	0.6	1.2	0.6
22	0.7	9.1	8.4
23	0.4	1.7	1.4
24	0.4	1.7	1.4
25	0.6	1.9	1.3
26	0.5	1.2	0.7
27	0.8	1.3	0.6
28	0.6	2.0	1.4
29	1.4	1.1	0.3
30	0.5	0.7	0.2
31	0.4	1.0	0.6
32	1.3	2.0	0.7
33	0.5	2.4	1.9
34	1.4	1.6	0.2
35	1.1	3.3	2.2
Mean	**0.6**	**1.5**	**0.9**
SD	**0.3**	**1.4**	**1.4**

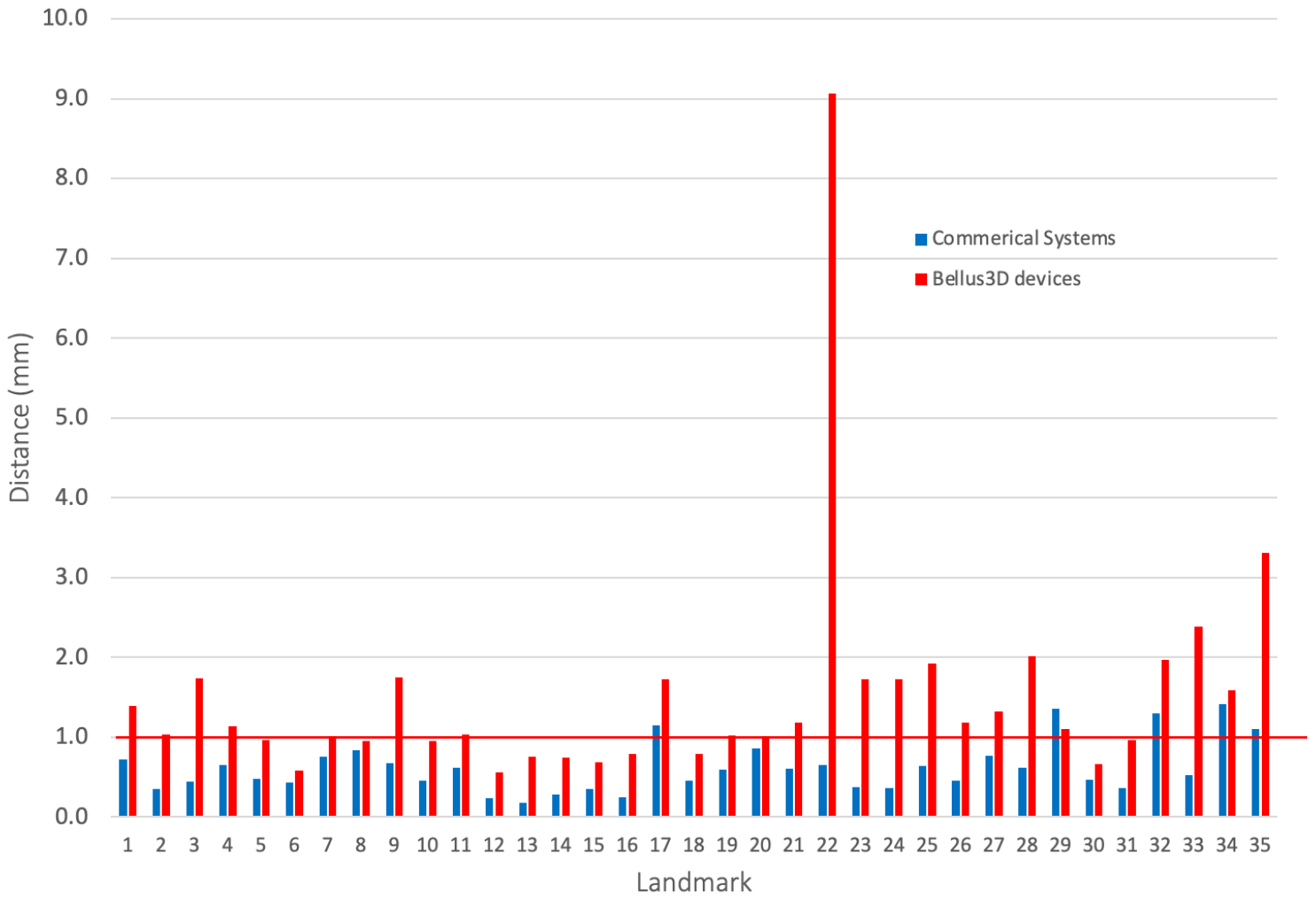

Figure 4.3 Mean Euclidean distance (mm) between the co-ordinate measuring machine (CMM) landmark and the Commercial systems and the Bellus3D devices. Red line at 1.0mm difference.

Table 4.3 Landmark error study based on the mean (±SD) absolute distances in the x, y and z-direction.

Landmark	x-direction		y-direction		z-direction	
	Mean (mm)	SD (mm)	Mean (mm)	SD (mm)	Mean (mm)	SD (mm)
1	0.20	0.15	0.26	0.31	0.17	0.14
2	0.27	0.15	0.23	0.17	0.05	0.04
3	0.33	0.31	0.29	0.20	0.32	0.42
4	0.14	0.16	0.34	0.29	0.17	0.16
5	0.20	0.23	0.36	0.25	0.06	0.06
6	0.35	0.26	0.19	0.13	0.34	0.27
7	0.18	0.19	0.20	0.10	0.21	0.18
8	0.37	0.18	0.24	0.17	0.05	0.03
9	0.15	0.18	0.13	0.09	0.17	0.19
10	0.19	0.14	0.19	0.15	0.09	0.09
11	0.20	0.12	0.33	0.14	0.13	0.11
12	0.07	0.09	0.27	0.21	0.15	0.09
13	0.27	0.16	0.24	0.14	0.13	0.13
14	0.28	0.24	0.19	0.17	0.12	0.14
15	0.22	0.16	0.30	0.13	0.12	0.07
16	0.29	0.18	0.22	0.20	0.06	0.05
17	0.24	0.26	0.28	0.22	0.16	0.23
18	0.15	0.12	0.22	0.18	0.35	0.17
19	0.24	0.17	0.24	0.19	0.21	0.22
20	0.29	0.19	0.21	0.13	0.07	0.08
21	0.27	0.26	0.17	0.14	0.10	0.11
Mean	0.23	0.07	0.24	0.06	0.15	0.09

4.3.2 Rest position stability

Table 4.4 shows that the reproducibility of the rest facial expression ranged from 0.5 ± 0.4mm for glabella (LM2) to 0.9mm ± 0.6mm for right forehead (LM1) and 0.9mm ± 0.5mm for right cheilion (LM13). The mean absolute differences in the x, y and z-directions were between 0.2mm and 0.5mm.

4.3.3 Bellus3d Face Camera Pro versus Di4D SNAP in rest position

Table 4.5 shows the mean absolute difference between the x, y and z-direction for Bellus3D Face Camera Pro and Di4D SNAP imaging systems for 21 landmarks (LM) when subjects were captured at rest. In the x-axis the greatest error (1.4 ± 0.9mm) was found at both the left and right gonion (LM12 and LM18). The next largest mean absolute error was seen in the right and left exocanthus areas (LM4 and LM6)., 1.0 ± 0.9mm and 1.0 ± 0.8mm respectively. The smallest mean absolute differences were seen in landmarks located along or close to the mid-facial region. In the y-axis the largest mean absolute difference of 1.0 ± 0.8mm was associated with the right forehead landmark (LM1) followed by pogonion (LM20) (0.9 ± 0.7mm) and menton (LM21) (0.9 ± 0.7mm) i.e., the most inferior landmarks located on the chin.

In the z-axis the largest mean absolute difference between Bellus3D Face Camera Pro and Di4D SNAP was 1.7 ± 1.6mm at right gonion (LM12), followed by 1.4 ± 1.1mm and 1.4 ± 1.2mm, associated with left gonion (LM18) and menton (LM21) respectively. These landmarks also displayed the highest variation.

Table 4.6 shows the mean Euclidean distance between the Bellus3D Face Camera Pro and Di4D SNAP imaging systems for 21 landmarks (LM) when subjects were

Table 4.4 Reproducibility of the mean (±SD) Euclidean and mean (±SD) absolute difference in the x, y and z-direction for rest position.

Landmark	**Euclidean distance**		**x-direction**	**y-direction**	**z-direction**
	Mean (mm)	SD (mm)	Absolute mean difference (mm)	Absolute mean difference (mm)	Absolute mean difference (mm)
1	0.9	0.6	0.4	0.5	0.4
2	0.5	0.4	0.2	0.3	0.2
3	0.7	0.6	0.3	0.3	0.5
4	0.6	0.4	0.2	0.2	0.4
5	0.7	0.3	0.3	0.5	0.2
6	0.6	0.3	0.3	0.3	0.3
7	0.7	0.5	0.4	0.3	0.3
8	0.7	0.3	0.3	0.5	0.3
9	0.8	0.3	0.5	0.3	0.5
10	0.6	0.2	0.3	0.4	0.3
11	0.6	0.3	0.4	0.3	0.2
12	0.7	0.3	0.3	0.3	0.5
13	0.9	0.5	0.4	0.5	0.5
14	0.6	0.3	0.3	0.3	0.3
15	0.7	0.3	0.3	0.4	0.3
16	0.7	0.4	0.3	0.4	0.4
17	0.8	0.3	0.5	0.5	0.5
18	0.7	0.4	0.2	0.3	0.5
19	0.6	0.3	0.3	0.3	0.3
20	0.6	0.3	0.2	0.3	0.3
21	0.7	0.2	0.3	0.5	0.3

Table 4.5 Mean (±SD) absolute difference in the x, y and z-direction between Bellus3D Face Camera Pro and Di4D SNAP imaging systems for 21 landmarks (LM) at rest.

Landmark	**x-direction**		**y-direction**		**z-direction**	
	Absolute mean difference (mm)	SD (mm)	Absolute mean difference (mm)	SD (mm)	Absolute mean difference (mm)	SD (mm)
1	0.6	0.5	1.0	0.8	0.5	0.4
2	0.3	0.2	0.7	0.5	0.4	0.3
3	0.5	0.4	0.8	0.5	0.7	0.6
4	1.0	0.9	0.8	0.5	0.6	0.4
5	0.4	0.3	0.6	0.6	0.3	0.2
6	1.0	0.8	0.4	0.4	0.7	0.4
7	0.5	0.5	0.4	0.4	0.6	0.4
8	0.4	0.3	0.5	0.4	0.4	0.3
9	0.8	0.7	0.4	0.4	0.6	0.5
10	0.4	0.3	0.4	0.3	0.9	0.5
11	0.5	0.3	0.4	0.4	0.8	0.5
12	1.4	0.9	0.6	0.6	1.7	1.6
13	0.6	0.4	0.6	0.5	0.6	0.4
14	0.4	0.2	0.4	0.3	0.5	0.4
15	0.4	0.3	0.4	0.3	0.6	0.4
16	0.4	0.3	0.5	0.3	0.6	0.4
17	0.6	0.5	0.7	0.4	0.7	0.5
18	1.4	0.9	0.6	0.6	1.4	1.1
19	0.4	0.3	0.6	0.4	0.6	0.5
20	0.3	0.2	0.9	0.7	0.5	0.4
21	0.4	0.3	0.9	0.6	1.4	1.2

Table 4.6 Mean (±SD) Euclidean distance between the Bellus3D Face Camera Pro and Di4D SNAP imaging systems for 21 landmarks (LM) when subjects were captured at rest.

Landmark	Absolute mean difference (mm)	SD (mm)	95% Confidence Intervals for mean difference (mm)		p-value
			Lower	Upper	
1	1.4	0.8	1.1	1.7	0.001*
2	1.0	0.4	0.8	1.1	0.001*
3	1.2	0.6	1.0	1.5	0.001*
4	1.6	0.8	1.3	1.9	0.008*
5	0.9	0.5	0.7	1.1	0.001*
6	1.4	0.7	1.2	1.7	0.001*
7	1.0	0.5	0.9	1.2	0.001*
8	0.9	0.4	0.8	1.1	0.001*
9	1.2	0.7	0.9	1.5	0.001*
10	1.1	0.4	0.9	1.2	0.001*
11	1.1	0.4	1.0	1.3	0.001*
12	2.5	1.7	1.9	3.1	0.945
13	1.2	0.6	1.0	1.4	0.001*
14	0.8	0.4	0.7	1.0	0.001*
15	0.9	0.5	0.7	1.1	0.001*
16	1.0	0.4	0.8	1.1	0.001*
17	1.3	0.5	1.1	1.4	0.001*
18	2.3	1.2	1.8	2.7	0.902
19	1.1	0.5	0.9	1.3	0.001*
20	1.2	0.6	1.0	1.5	0.001*
21	1.9	1.1	1.5	2.4	0.376

One-sample t-test with a hypothesised mean of 2.0mm

*Significantly less than 2.0mm

captured at rest. Left and right gonion (LM12 and LM18) had the greatest distance between landmarks, both greater than 2.0mm, at 2.5 ± 1.7mm and 2.3 ± 1.2mm respectively. Eighteen of the twenty-one landmarks had an average Euclidean distance of 2mm or less, and all of these were located on or near to the mid facial axis.

Based on a one-sample *t*-test determining whether the mean Euclidean distance between the Bellus3D Face Camera Pro and Di4D SNAP 3D configurations were statistically significantly different to a hypothesised mean distance of 2.0mm, three landmarks, right and left gonion and menton (LM12, LM18 and LM21) had an average Euclidean distance which were not statistically significantly different to 2.0mm. The remaining landmarks were statistically significantly less than 2.0mm. Only one landmark right philtrum (LM14), was found to have a mean Euclidean distance, between the Bellus3D Face Camera Pro and Di4D SNAP 3D configurations, statistically significantly less than 1.0mm. Figure 4.4 and 4.5.

4.3.4 Bellus3d Face Camera Pro versus Di4D SNAP at maximum smile

Table 4.7 shows the mean absolute difference between the Bellus3D Face Camera Pro and Di4D SNAP imaging systems for 21 landmarks when subjects were captured at maximum smile. In the x-axis, the largest error (1.4 ± 1.1mm) was at left exocanthus (LM6) and left gonion (LM18, 1.4 ± 1.1mm). The next largest mean absolute differences were seen on the right hand side of the face at the exocanthus, gonion, and philtrum (landmarks 4, 12 and 13) 1.2 ± 0.9mm, 1.1 ± 0.7mm and 1.1 ± 0.8mm respectively. The smallest mean absolute differences were seen in landmarks located along or close to the mid-facial region above the upper lip. In the y-axis the largest

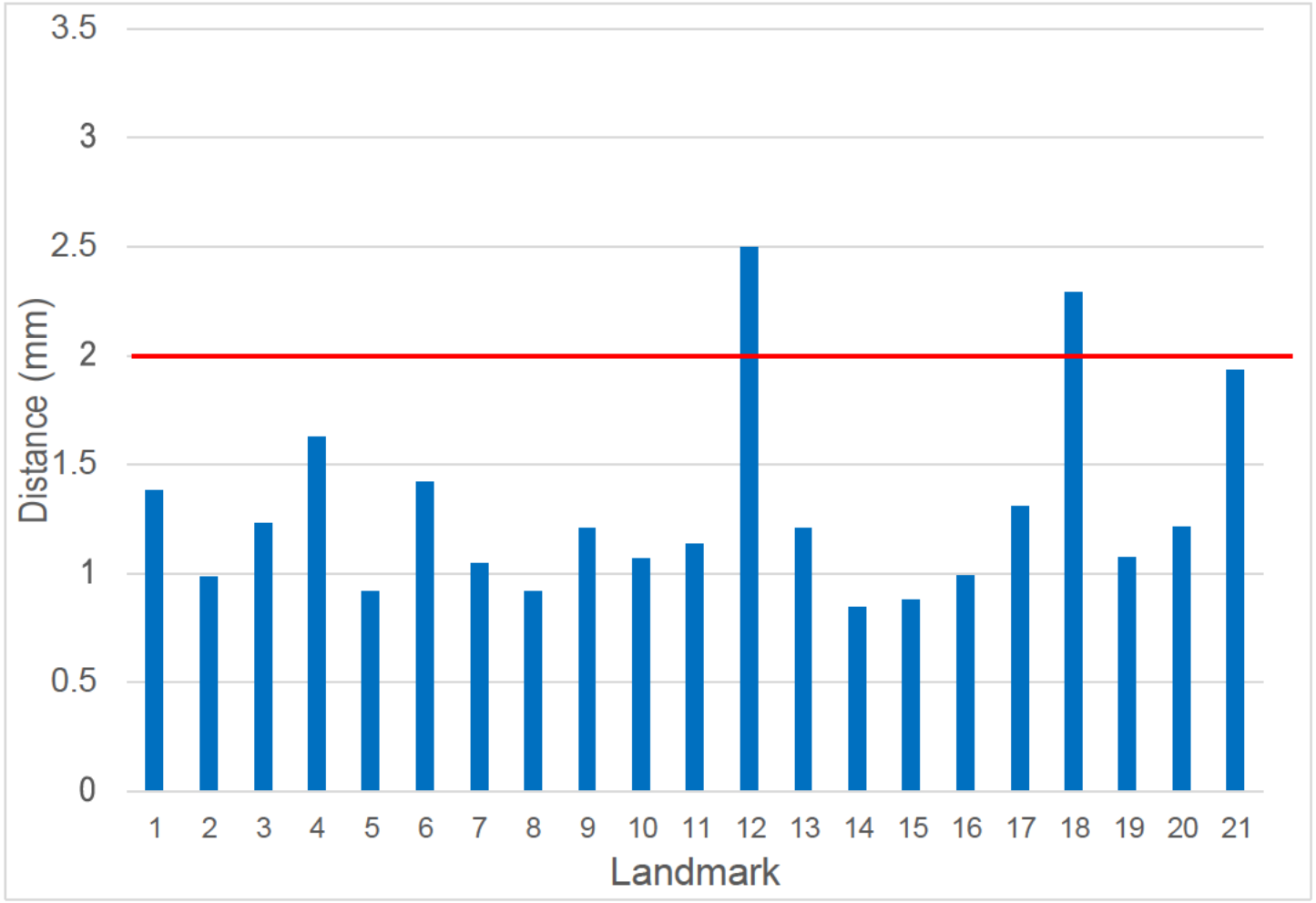

Figure 4.4 Mean Euclidean distance (mm) between the Di4D SNAP landmarks and the Bellus3D Face Camera Pro at rest. Red line at 2.0mm difference.

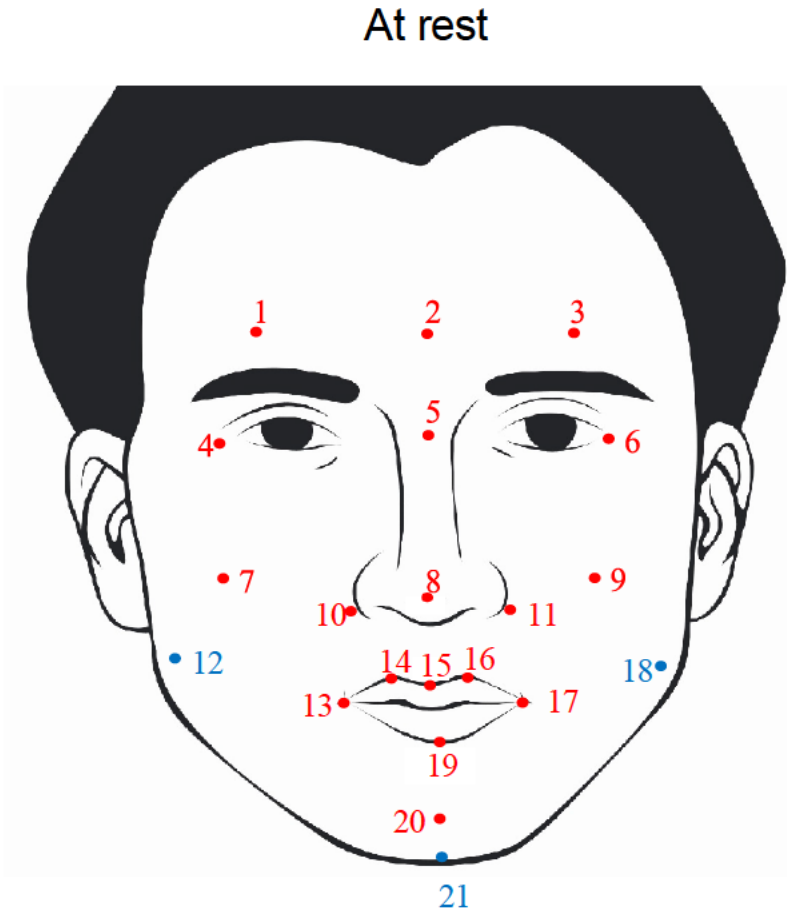

Figure 4.5 Diagram showing landmarks (in RED) where the mean Euclidean distances between the Bellus3D Face Camera Pro and Di4D SNAP 3D configurations are statistically significantly less than 2.0mm.

Table 4.7 Mean (±SD) absolute difference in the x, y and z-direction between Bellus3D Face Camera Pro and Di4D SNAP imaging systems for 21 landmarks (LM) at maximum smile.

Landmark	**x-direction**		**y-direction**		**z-direction**	
	Absolute mean difference (mm)	SD (mm)	Absolute mean difference (mm)	SD (mm)	Absolute mean difference (mm)	SD (mm)
1	0.5	0.4	1.0	0.9	0.7	0.6
2	0.4	0.3	0.9	0.6	0.5	0.4
3	0.4	0.5	0.9	0.6	0.8	0.7
4	1.2	0.9	0.7	0.6	1.0	0.7
5	0.4	0.3	0.6	0.5	0.4	0.3
6	1.4	1.1	0.6	0.5	1.4	0.9
7	0.9	0.7	0.6	0.6	0.9	0.9
8	0.4	0.4	0.6	0.4	0.5	0.4
9	0.8	0.6	0.6	0.6	0.6	0.6
10	0.6	0.5	0.6	0.5	1.1	0.8
11	0.6	0.5	0.6	0.6	1.1	0.8
12	1.1	0.7	0.9	0.7	2.2	1.6
13	1.1	0.8	0.7	0.7	1.6	1.1
14	0.5	0.4	0.4	0.4	0.6	0.4
15	0.4	0.3	0.5	0.4	0.6	0.4
16	0.5	0.5	0.4	0.2	0.7	0.4
17	0.8	0.7	0.9	0.8	1.6	1.2
18	1.4	1.1	1.3	0.7	2.3	1.8
19	0.5	0.3	0.9	0.7	0.6	0.5
20	0.4	0.3	1.1	0.7	0.8	0.6
21	0.5	0.6	1.7	1.5	1.4	1.5

mean absolute difference of 1.7 ± 1.5mm was at menton (LM21). In the z-axis the largest mean absolute differences between Bellus3D Face Camera Pro and Di4D SNAP were 2.3 ± 1.8mm at left gonion (LM18), and 2.2 ± 1.6mm for right gonion (LM12). Left gonion (LM18), displayed the highest variation with a standard deviation of 1.8mm.

Table 4.8 shows the mean Euclidean distance between the Bellus3D Face Camera Pro and Di4D SNAP imaging systems for 21 landmarks (LM) when subjects were captured at maximum smile. Left and right gonion had the greatest Euclidean distance between (LM12 and LM18) both were greater than 2.0mm at 2.8 ± 1.2mm and 3.3 ±1.9mm respectively.

Based on a one-sample *t*-test determining whether the mean Euclidean distance between the Bellus3D Face Camera Pro and Di4D SNAP 3D configurations were statistically significantly different to a hypothesised mean distance of 2.0mm, seven landmarks, right and left exocanthus, left and right gonion, left and right cheilion and menton (LM4, LM6, LM12, LM13, LM17, LM18 and LM21) had an average Euclidean distance which were not statistically significantly different to 2.0mm, Figure 4.7. The remaining landmarks were statistically significantly less than 2.0mm. No landmarks were found to have a mean Euclidean distance, between the Bellus3D Face Camera Pro and Di4D SNAP 3D configurations, statistically significantly less than 1.0mm at maximum smile.

Table 4.8 Mean (±SD) Euclidean distance between the direction for Bellus3D Face Camera Pro and Di4D SNAP imaging systems for 21 landmarks (LM) at maximum smile.

Landmark	Absolute mean difference (mm)	SD (mm)	95% Confidence Intervals for mean difference (mm)		p-value
			Lower	Upper	
1	1.5	0.9	1.1	1.8	0.002*
2	1.2	0.6	1.0	1.4	0.001*
3	1.4	0.8	1.1	1.7	0.001*
4	1.9	1.0	1.5	2.2	0.245
5	1.0	0.5	0.8	1.1	0.001*
6	2.3	1.1	1.9	2.7	0.924
7	1.6	0.9	1.3	2.0	0.022*
8	1.0	0.4	0.8	1.2	0.001*
9	1.4	0.8	1.1	1.7	0.001*
10	1.6	0.9	1.2	1.9	0.006*
11	1.6	0.9	1.3	1.9	0.009*
12	2.8	1.6	2.2	3.4	0.996
13	2.3	1.2	1.8	2.7	0.889
14	1.0	0.4	0.9	1.2	0.001*
15	1.0	0.4	0.9	1.2	0.001*
16	1.0	0.4	0.9	1.2	0.001*
17	2.2	1.2	1.7	2.7	0.799
18	3.3	1.8	2.6	3.9	1.000
19	1.4	0.6	1.2	1.6	0.001*
20	1.6	0.7	1.3	1.9	0.002*
21	2.3	1.9	1.6	3.1	0.806

One-sample t-test with a hypothesised mean of 2.0mm.

*Significantly less than 2.0mm

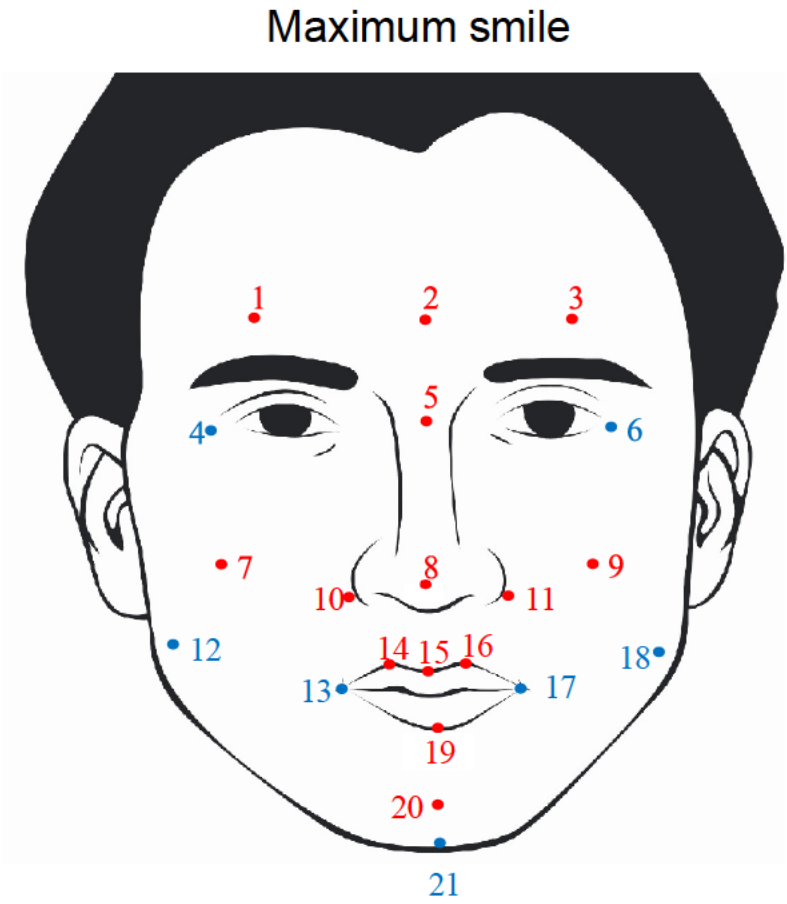

Figure 4.6 Diagram showing Landmarks (in RED) where the mean Euclidean distances between the Bellus3D Face Camera Pro and Di4D SNAP 3D configurations are statistically significantly less than 2.0mm.

CHAPTER 5

DISCUSSION

5.1 DISCUSSION

Technology developed for one particular purpose is often be adapted for alternative uses, for example the camera system incorporated into some Apple products. The complex array of cameras, a standard feature of many devices, recognises the face in three-dimensions (3D) as a means of “unlocking” the device, can also be used to generate a 3D facial image. The same can be said for fingerprint recognition systems. These forms of security systems were once only found in government agencies. Technological advances have meant that devices that were once only commercially available are now “pocket sized” and easily at hand.

The first part of this study was an in vitro investigation assessing the validity and accuracy of two commercially available 3D images systems, 3dMD and Di4D SNAP, and two versions of the Bellus3D (Bellus3D Face Camera Pro and Bellus3D iPhone App) against a gold standard Co-ordinate Measuring Machine (CMM). In this study a plastic mannequin head was used as it closely represented a human face, with regards to shape and texture but was rigid and totally static and therefore a stable object or subject. The CMM was taken as the gold standard as it measures the geometry of an object by measuring discrete points on the surface using a probe. The movement of the probe is along three axes that are orthogonal to one another. Each axis has a sensor that records the position of the probe relative to an origin, with accuracy in the order of microns. The use of the mannequin head and CMM provided the “ideal” environment to assess the validity and accuracy of the four capture devices. The CMM recorded the x, y and z positions of each landmark in a three-dimensional (3D) Cartesian coordinate system. When all 35

landmarks were identified on the mannequin head, a 3D landmark configuration was produced, and it was this which was used for analysis.

5.2 Methods of analysis

Several methods of analysis have been described in the literature, these include surface mesh analysis based on colour maps or heat maps, point-to-point measurements, or linear Euclidean measurements. There are advantages and short comings of the different methods of analysis. Several studies have superimposed the facial mesh data, using the iterative closest point (ICP) algorithm which aligns the two different meshes as close as possible, and then measures the Euclidean distance between the two meshes (Gallardo *et al.*, 2021). The validity of this method is questionable since measurement between meshes are based on nearest points, not on corresponding anatomical points (Jabar *et al.*, 2015). Thus, any two images of a similar shape may show a high level of concordance even though they are unrelated. In addition, with reference to the entire face significant differences in specific regions of the face will be diluted by the thousands of points that show very little differences. This will greatly under-estimate the magnitude of any error. Another shortcoming of this method of analysis is that a single mean difference between two facial meshes cannot describe the error across the entire face and is therefore not clinically meaningful or relevant. In an attempt to address this shortcoming, some studies have divided the face into regions of interest, made up of fewer points, but again the differences are based on the mean absolute deviation between all the nearest points and not the anatomically corresponding points.

The use of point-to-point measurements can also be associated with problems. Following superimposition of the two facial meshes, the operator can select a point on one mesh and the software automatically calculates the Euclidean distance between the two meshes, based on the nearest point on the second mesh, which as mentioned above may not be clinically valid. An alternative option is to physically choose anatomically corresponding landmark on both facial meshes and determine the Euclidean distance between them. This relies on the operator being able to identify the same landmarks on both images with a high level of accuracy and precision. Studies using this technique should report the landmark identification error as well as the difference between the landmarks. This will differentiate true differences from errors in identifying landmarks.

The use of linear measurements is also associated with errors. A simple linear measurement is dependent on only two points; there is a chance that two points can be incorrectly identified in 2D space but the distance between them remains the same. For example, if the distance between two points is measured at 20mm at T_1, but at T_2 the two points are both 5mm to the left, the distance between them is the same (20mm), however they may not be measuring the same physical structure on both occasions. The situation is even more complex in 3D as now depth also has an effect. For example, if the distance between two points is measured at 20mm at T_1, but at T_2 one of the points is 5mm behind the original point, the distance between them is approximately the same (20mm), but again they may not be measuring the same physical structure on both occasions. The use of simple linear distances in 3D space may not necessarily represent the true clinical measurements of the chosen points.

Accepting the problems with mesh analysis and point to point measurements the present study used specific landmarks distributed over the face extending from ear to ear in width and from the forehead to the chin vertically. To reduce on-screen landmarking error the subjects were physically pre-landmarked with by placing marks directly on the subject's face. This meant that the on-screen landmark identification and digitisation would be reduced to a minimum. Having landmarked each face, the 3D landmark configurations for each image could then be compared. Comparison was achieved by using Partial Procrustes superimposition where any two 3D configurations could be compared by rotating and translating them until the "best-fit" was achieved. Having achieved the best fit the Euclidean distances between all the corresponding landmarks could be calculated. The advantage of this method of analysis was that differences between anatomically corresponding landmarks were directly calculated. However, a short coming is that any landmarks that are grossly incorrect would "pull" one 3D configuration away from the other, known as the "Pinocchio effect".

5.3 In vitro study

A previous study has cited that a difference of 1mm (Euclidean distance) between standard anthropometric measurements and 3D images captured using a laser scanner were considered highly reliable measurements (Aung *et al.,* 1995). The same threshold has been used by previous studies to assess Bellus3D (Gallardo *et al.*, 2021; Liu *et al.*, 2021; Pan *et al.*, 2022).

The present in vitro study found that for both 3dMD and Di4D SNAP many landmarks were on accurate to within 1mm of the CMM landmarks under ideal conditions. Apart from

left cheilion, the least accurate landmarks (>1mm) were located laterally. The different methods of analysis make direct comparison with other studies difficult. However for Di4D SNAP the results of the present study are consistent with previous validation studies of Di3D, an earlier version Di4D SNAP, with an error of around 0.3mm (Khambay *et al.*, 2008). The study used a similar gold standard, CMM and the same method of analysis based on the 3D landmark configuration. Only 10 landmarks were used, opposed to the 35 used in the present study, in addition, the majority of the 10 landmarks were centrally placed in the face. This may explain the slightly larger error of 0.6 ± 0.3mm found in the present study when comparing Di4D SNAP to the CMM landmark positions. The error for 3dMD in the present study, 0.7 ± 0.3mm, was found to be larger than previously shown, 0.01 ± 0.55mm (Lübbers *et al.*, 2010). The reason for this maybe that direct anthropometric linear measurement between landmarks was used, opposed to direct landmark differences using a CMM. Both the 3dMD and Di4D SNAP systems were clinically comparable to one another.

Both the Bellus3D systems were less accurate than the commercial systems (Di4D SNAP and 3dMD). Over half the landmarks showed a mean difference greater than 1mm from the CMM landmark positions. The Bellus3D Face Camera Pro was as accurate as the Bellus3D iPhone App, however the mean accuracy of both systems was significantly more than 1mm. Soft tissue menton (LM 22) showed the largest magnitude of error, as well inferior or laterally located landmarks. This was probably due to the face / head being curved and having to rotate around a fixed point. The camera is taking two-dimensional “flat” images of a curved surface and trying to construct the curvature and restoring depth.

Since changes in subject facial expression were impossible, the difference in the observed accuracy between the 3D imaging systems and the CMM must be due to the inherent system capture error. Landmarking error was minimum for this study as a result of pre-landmarking the face. The commercial systems comprised of three pairs of cameras located in front, to the right and to the left of the subject. The lower cameras were located so that they capture from a slightly inferior angle, allowing for capture of the inferior and lateral areas of the face. The Bellus3D Face Camera Pro and Bellus3D Face App use superiorly and centrally located cameras, causing difficulties in capturing inferior landmarks. Previous in vitro studies have compared the Bellus3D systems to direct anthropometric measurements of linear distances between landmarks (Liu *et al.*, 2021; Pan *et al.*, 2022). The reported results were more accurate than the present findings, however the methods of analysis between studies was not comparable. Both the Bellus3D Face Camera Pro and Bellus3D Face App systems were clinically comparable to one another. However, the commercial systems were superior to the Bellus3D systems, with a mean difference in Euclidean distance of 0.9 ± 1.4mm between them, this was statistically significant ($p = 0.001$) and clinically significant with a 95% confidence interval for the difference of -1.4mm to -0.4mm.

5.4 In vivo study

The in vivo study showed that even though the commercial capture systems had a higher degree of accuracy compared to the Bellus3D Face Camera Pro, the magnitude of the error, around 1.0mm, was a difference that may be clinically acceptable. Therefore an in vivo study was undertaken to determine the validity and accuracy of Bellus3D Face Camera Pro compared to Di4D SNAP whilst capturing human faces at rest and at

maximum smile. Facial expressions are an important form of non-verbal communication with studies suggesting that 80% of communication is nonverbal and 20% verbal (Hull, 2016). While nonverbal communication varies between cultures, the basic facial expressions for happiness, sadness, anger, and fear are all similar. Capturing a facial smile in 3D is fundamental for aesthetic purposes, e.g., the identification of key muscle groups as targets for Botox® in an asymmetric or gummy smiles, as a guide for smile re-animation in patients who have suffered facial palsy (Sun *et al.,* 2022) or during digital smile design. As with facial scans at rest, comparisons can be made pre- and post-treatment to evaluate the effects of the intervention, such as re-innervation surgery or facelift surgery (Li, *et al.,* 2015; Gibelli *et al.,* 2020). No studies to date have assessed the accuracy of using Bellus3D to capture maximum smiles. The ability of using “at-hand” devices and software to capture a maximum smile for digital smile design opens up the use of 3D technology for routine clinical use. Capturing a smile with Di4D SNAP is potentially easier and more accurate as the individual smiles and the left and right of the face is captured simultaneously, in 1/500 of second, but more expensive. However, when using Bellus3D to capture maximum smile, the individual would need to hold maximum smile whilst moving their head from left and right over a much longer period (15 seconds). This introduces fatigue and the possibility of motion artifacts. This study was undertaken to determine if this difference was clinically significant.

Interestingly, previous studies have used a larger limit of 2mm difference between the control and the experimental system for clinical use (Aung *et al.,* 1995; Knoops *et al.,* 2017; Artopoulos *et al.,* 2014; Maués *et al.,* 2018; Andrews *et al.,* 2023; Camison *et al.,* 2018). Differences of between 1mm to 3mm have been suggested as being acceptable

for clinical application (D'Ettorre *et al.,* 2022; Thurzo *et al.,* 2022). Given that the majority of studies have used a 2mm difference between the control and the experimental system as their level of acceptability this was adopted in the present investigation. This 2mm difference will be made up of several sources of error including, capture error and landmarking error. The study was interested in capture error i.e., the error inherent in each capture system whilst ensuring landmarking error was as low as possible; this was achieved by pre-landmarking 21 landmarks on to each individual and then capturing their faces using Di4D SNAP and Bellus3D.

Pre-landmarking reduced the error associated with digital on-screen landmarking, this was particularly important for less well-defined anatomical landmarks such as gonion or landmarks around the cheek region. The landmarking software allowed for magnification and rotation of the image to visualise and identify each landmark. For the present study repeatability of intra-examiner landmarking was found to be consistent, with the mean error found to be less than 0.25mm in all directions, this was similar or superior to the findings of previous studies (D'Ettorre *et al.,* 2022; Aljawad *et al.,* 2022; Nord *et al.,* 2015; Aldridge *et al.,* 2005; Wong *et al.,* 2008). As well as assessing landmark identification error, rest position reproducibility was assessed; the mean absolute differences in the x, y and z- directions were found to be between 0.2mm and 0.5mm. This was similar to Johnstone et al. (2003) who reported an average variation in overall land-mark position of 0.74 mm between rest positions (Johnston *et al.,* 2003). Maximal smile has previously been shown to have the least difference in magnitude and speed between two time intervals compared to other facial expressions (Ju *et al.,* 2018).

At rest the absolute mean Euclidean difference between DiD4 SNAP and the Bellus3D Face Camera Pro was statistically significantly 2.0mm or less than for 18 of the 21 landmarks, and 1.0mm or below for 7 of the 21 landmarks. The largest error was at right and left gonion and soft tissue menton; all the landmarks with the least error were in the region adjacent to the facial midline. Based on the 95% confidence the mean Euclidean difference between DiD4 SNAP and the Bellus3D Face Camera Pro was not significantly clinically different (more than 2.0mm) for all landmarks except right and left gonion and soft tissue menton, where the upper limits exceeded 2.0mm. When decomposed into the separate x, y and z directions, only 3 of 21 landmark had differences that exceeded 1.0mm. These were again right and left gonion in the x and z direction and menton in the z direction. The difference observed between the DiD4 SNAP and the Bellus3D Face Camera Pro for menton may be due to the difference in camera location between the systems, and the fact that Bellus3D is unable to capture under the chin as the individual is encouraged to look ahead into the camera, whilst with Di4D SNAP the head is often tilted back slightly. For left and right gonion as the subject is instructed to rotate their head from left to right using Bellus3D there will be some stretch and soft tissue distortion in the neck / angle of mandible region, whilst Di4D SNAP takes a single static image.

At maximum smile the absolute mean Euclidean difference was significantly below 2.0mm for 14 of the 21 landmarks. In addition to gonion and menton, landmarks right and left exocanthion and right and left and cheilion were greater than 2.0mm. This is most likely because these areas are subject to most movement during smile and holding this strained position would be difficult for the entire Bellus3D Face Camera Pro scanning time. This suggests that there are two sources of error using Bellus3D over Di4D SNAP. The first is

the inherent error present within each device, but error at rest has found that this only relates to left and right gonion and menton. The second error is the error associated with holding the maximum smile expression over a 15 second period. Previous studies have shown smiling to be reducible, but these have been a “snapshot” of the smile. Thus, the present study has shown that maintaining maximum smile whilst using Bellus3D introduces additional errors at the corners of the mouth and the eye, the areas which displace the most during smiling. These results are confirmed in previous studies, as maximum smile has previously been found to be less reliable than rest position, and increased error was also found in the same additional areas with smile (periorbital and cheilion) (Johnston *et al.,* 2003; Sawyer *et al.,* 2009).

The method of analysis and the outcome measure used will have an impact on conclusions reached by each study. Many in vivo studies use inter-landmark differences as the outcome measure. This is based on historical anthropometric measurement techniques and likely due to the convenience of only requiring a digital calliper. However as mentioned earlier a simple linear measurement of inter-landmark distances is dependent on only two points; there is a chance that two points can be incorrectly identified in 2D space but the distance between them remains the same. This would give the false impression that the accuracy was acceptable. Many of the previous studies found average differences between Bellus3D and direct anthropometry to be within 1mm (Piedra-Cascón *et al.,* 2020; Raffone, *et al.,* 2022). Piedra-Cascón et al. (2020) was limited to inter-landmark differences in the midface, whilst Raffone et al. (2022) did not use measurements involving menton. These methodical differences could account for some of the differences seen with the present study. In a study assessing the accuracy of both

Bellus3D Face App and a new multi-camera version of Bellus3D (Bellus3D ARC1), the former was accurate to slightly above 1mm and the latter slightly below, the authors attributed this finding to the enhanced hardware (Wang *et al.*, 2021). However, higher differences (21 of 23 linear measurements within 1.5mm) were seen in a study comparing Bellus3D ARC1 to segmented surface CBCT scan (Aljawad *et al.,* 2022). The landmark locations are not specified therefore no comparisons can be drawn and the threshold values / segmentation process selected during conversion of DICOM CBCT data to surface files may alter the dimensions of the “gold-standard” 3D surface model.

As an alternative to direct anthropometric measurement, a second scanning system is often used as a control, in which case the 3D surface meshes can be compared. As discussed previously the analysis based on colour maps or heat maps, point-to-point measurements, or linear Euclidean measurements, has the potential of reducing the true error (D'Ettorre *et al.*, 2022; Aljawad et al., 2022; Andrews *et al.*, 2023). One study used sectional surface mesh comparisons of 21 facial areas of Bellus3D Face app and segmented surface CBCT scans (Thurzo *et al.*, 2022). Generally increased deviation was seen in the lateral facial areas (temporal and gonial) which is consistent with our findings, but also in the lower lip and peri oral areas, likely due to changes in micro expression due to the long scanning time of CBCT.

Only two studies compared absolute landmark location using point-to-point measurement, where following superimposition of the two facial meshes, the operator selects a point on one mesh and the software automatically selects the nearest point on the second mesh and calculates the Euclidean distance between the two which as mentioned above may

not be clinically valid (D'Ettorre *et al.*, 2022; Andrews *et al.*, 2023). D'Ettorre et al. (2022) reported 13 of 18 landmarks were within 1mm of the reference landmarks (D'Ettorre *et al.*, 2022). The least accurate results were found in endocanthus and cheilion, possibly due to shadowing and change in micro-expression respectively. Gonion and menton were included but conversely to our findings had good or average results. The second study found 16 landmarks to be within 1mm of the reference landmarks (Andrews *et al.*, 2023). As with our findings most error was found in the lateral areas (gonion and traigon) and the least in areas close to the midline. The present study used differences in distances based on anatomical correspondence rather than the nearest point, this may explain the reason both studies found Bellus3D to be more accurate than in the present study.

Digital dentistry is progressing rapidly due to increased aesthetic demands from patients and is facilitated by advancing technology (Shepperson, 2023). Smart phone technology is ubiquitous in most aspects of modern life and dentistry is no exception, smile design can be completed virtually using easily accessible specialised apps. Digital oral scans are replacing conventional plaster models and can be combined with 2D or 3D facial photographs to produce a digital patient (Finelle, 2017), providing information usually lacking in conventional planning methods such as tooth show at rest and at smile, lip mobility, and the harmony of the aesthetic dentition relative to the patients face as a whole (Jreige *et al.,* 2022).

Specialised software applications allow simulation of various treatment plans. It is possible to simulate orthodontic tooth movement, gingival modifications and restorative treatments, to achieve ideal aesthetics in terms of gingival zenith position, tooth proportions, colour

and smile arc. The outcomes can be 3D printed and used as templates for intra-oral mockups, improving the communication of realistic end goals with both the patient and the dental laboratory (Shepperson, 2023).

Bellus3D Face Camera Pro was shown to be accurate for clinical use in the facial midline and the adjacent areas including the mouth and lips at rest and at maximum smile, apart from left and right cheilion. As such, it offers a more accessible alternative, both logistically and financially, to conventional 3D imaging systems for dental practitioners interested in 3D smile design. Due to the variable position of cheilion in the scanning process of maximum smile, Bellus3D Face Camera Pro derived images may provide problems planning cases where buccal corridor modification is required.

CHAPTER 6

CONCLUSIONS

6.1 IN VITRO

The null hypothesis is rejected

The null hypothesis is rejected. There was a statistically significant difference ($p<0.05$) in the position (based on the Euclidean distance) of 35 facial landmarks, captured using the Bellus3D devices and the commercial systems.

6.2 IN VIVO

The null hypothesis is rejected

For all landmarks, except right and left gonion and menton, the null hypothesis is rejected. The mean differences in Euclidean distance, capturing the face at rest, using Bellus3D Face Camera Pro and Di4D SNAP, were statistically significantly ($p<0.05$) less than the hypothesised clinically significant mean distance of 2.0mm.

For all landmarks, except right and left gonion, right and left exocanthion and menton, the null hypothesis is rejected. The mean differences in Euclidean distance, capturing the face at maximum smile, using Bellus3D Face Camera Pro and Di4D SNAP, was statistically significantly ($p<0.05$) less than the hypothesised clinically significant mean distance of 2.0mm.

6.3 CLINICAL IMPLICATIONS

- At rest, the Bellus3D Face Camera Pro was accurate to within 2.0mm of Di4D for 18 of 21 landmarks, except right and left gonion and menton.
- At maximum smile, the Bellus3D Face Camera Pro was accurate to within 2.0mm of Di4D for 14 of 21 landmarks, except right and left gonion, right and left cheilion, right and left exocanthion and menton.

- The largest errors were in inferior or lateral regions of the face.
- The lowest errors were seen in landmarks closer to the middle of the face.
- Bellus3D Face Camera Pro is suitable for clinical application if limited to areas adjacent to the midline in rest and maximum smile.
- Bellus3D Face Camera Pro is not suitable for clinical use where investigation of lateral and inferior areas of the face is required, nor for transverse smile investigation.

CHAPTER 7

REFERENCES

7.1 REFERENCES

Akan, B. and Veli, I. (2020) Evaluation of soft-tissue changes in young adults treated with the Forsus fatigue-resistant device. *American Journal of Orthodontics and Dentofacial Orthopedics*, 157 (4): 481-489.

Al-Rudainy, D., Ju, X., Mehendale, F., and Ayoub, A. (2018) Assessment of facial asymmetry before and after the surgical repair of cleft lip in unilateral cleft lip and palate cases. *International Journal of Oral and Maxillofacial Surgery*, 47 (3): 411–419.

Aldridge, K., Boyadjiev, S.A., Capone, G.T., DeLeon, V.B., and Richtsmeier, J.T. (2005) Precision and error of three-dimensional phenotypic measures acquired from 3dMD photogrammetric images. *American Journal of Medical Genetics*, 138 (3): 247–253.

Aljawad, H., Lim, H.-J. and Lee, K.C. (2022) Anthropometric Comparison of 3-Dimensional Facial Scan Taken With a Low-Cost Facial Scanner With Cone-Beam Computed Tomography Scan. *Journal of Craniofacial Surgery*, 34 (5): 1456-1458.

Andrews, J., Alwafi, A., Bichu, Y.M., Pliska, B.T., Mostafa, N. and Zou, B (2023) Validation of three-dimensional facial imaging captured with smartphone-based photogrammetry application in comparison to stereophotogrammetry system. *Heilyon,* 9 (5): e15834.

Artopoulos, A., Buytaert, J.A.N., Dirckx, J.J.J., Coward, T.J. (2014) Comparison of the accuracy of digital stereophotogrammetry and projection moiré profilometry for three-dimensional imaging of the face. *International Journal of Oral and Maxillofacial Surgery,* 43 (5): 654–662.

Aung, S.C., Ngim, R.C.K. and Lee, S.T. (1995) Evaluation of the laser scanner as a surface measuring tool and its accuracy compared with direct facial anthropometric measurements. *British Journal of Plastic Surgery*, 48 (8): 551–558.

Ayoub, A., Siebert, P., Moos, K.F., Wray, D., Urquhart, C. and Niblett, T.B. (1998) A vision-based three-dimensional capture system for maxillofacial assessment and surgical planning. *Surgery,* 36 (5): 353-357.

Beri, A., Pisulkar, S.K., Bagde, A.D., Bansod, A., Dahihandekar, C. and Paikaro, B. (2022) Evaluation of accuracy of photogrammetry with 3D scanning and conventional impression method for craniomaxillofacial defects using a software analysis. *Trials*, 23 (1): 1-10.

Bird, J.M. (1982) Computerized Tomograpy, Atrophy and Dimentia: A Review. *Progress in Neurobiology*, 19 (1-2): 91-115.

Bockstedte, M., Xepapadeasa A.B., Spintzyk, S., Poets, C.F., Koos, B. and Aretxabaleta, M. (2022) Development of Personalized Non-Invasive Ventilation Interfaces for Neonatal and Pediatric Application Using Additive Manufacturing. *Journal of Personalised Medicine,* 12 (4): 604-619.

Camison, L., Bykowski, M., Lee, W.W., Carlson, J.C., Roosenboom, J., Goldstein, J.A., Losee, J.E. and Weinberg, S.M. (2018) Validation of the Vectra H1 portable three-dimensional photogrammetry system for facial imaging. *International Journal of Oral and Maxillofacial Surgery*, 47 (3): 403–410.

Carter, J.L., Patel, A., Hocum, G. and Benninger, B. (2017) Thyroid gland visualization with 3D/4D ultrasound: integrated hands-on imaging in anatomical dissection laboratory. *Surgical and radiologic anatomy,* 39 (5): 567–572.

Carter, L.N., Reed, C.A., Morrell, A.P., Fong, A.K.H., Chowdhury, R., Miller, E., Alberini, F., Khambay, B., Anand, S., Grover, L.M., Coward, T., Addison, O. and Cox, S.C. (2021) Three dimensional analysis of the face in respect of zygomatic fractures and evaluation of the surgery with the aid of Moiré topography. *Scientific Reports,* 11 (1): 21449

Chang, F.C.S., Wallace, C.G., Hsiao Y.C., Huang J.J., Liu, C.S.W., Chen, Z.C., Chen, P.K.T., Chen, J.P. and Chen, Y.R. (2020) Long-term comparison study of philtral ridge morphology with two different techniques of philtral reconstruction. *International Journal of Oral and Maxillofacial Surgery*, 49 (10): 1254–1259.

Cho, M-J., Hallac, R.R., Ramesh, J., Seaward, J.R., Hermann, N.V., Darvaan, T.A., Lipira, A. and Kane, A.A. (2018) Quantifying normal craniofacial form and baseline craniofacial asymmetry in the paediatric population. *Plastic and reconstructive Surgery,* 141 (3): 380e-387e.

Codari, M., Puccuarelli, L., Pisoni, L. and Sforza, C. (2015) Laser scanner compared with stereophotogrammetry for measurements of area on nasal plaster casts. *British Journal of Oral and Maxillofacial Surgery*, 53 (8): 769–770.

Demir, R. and Baysal, A. (2020) Three-dimensional evaluation of smile characteristics in subjects with increased vertical facial dimensions. *American Journal of Orthodontics and Dentofacial Orthopedics,* 157 (6): 773-782.

De Stefani, A., Barone, M., Alamdari, S.H., Barjami, A., Baciliero, U., Apolloni, F., Gracco, A. and Bruno, G. (2022) Validation of Vectra 3D Imaging Systems: A review. *International Journal of Environmental Research and Public Health,* 19 (14): 8820-8833.

D'Ettorre, G.D., Farronato, M., Candida, E., Quinzi, V. and Grippaudo, C. (2022) A comparison between stereophotogrammetry and smartphone structured light technology for three-dimensional face scanning. *Angle Orthodontist*, 92 (3): 358–363.

Dindaroğlu, F., Duran, G.S., Görgülü, S. and Yetkiner, E. (2016) Social smile reproducibility using 3-D stereophotogrammetry and reverse engineering technology. *Angle Orthodontist,* 86 (3): 448-455.

Dindaroğlu, F., Kutlu, P., Duran, G.S., Görgülü, S. and Aslan, E. (2016) Accuracy and reliability of 3D stereophotogrammetry: A comparison to direct anthropometry and 2D photogrammetry. *Angle Orthodontist*, 86 (3): 487–494.

Dirckx, J.J.J., Buytaert, J.A.N. and Van der Jeught, S.A.M. (2010) Implementation of a phase-shifting moirè profilometry on a low-cost commercial data projector. *Optics and Lasers in Engineering,* 48 (2): 244-250.

Dobreva, D., Gkantidis, N., Halazonetis, D., Verna, C. and Kanavakis G. (2022) Smile Reproducibility and Its Relationship to Self-Perceived Smile Attractiveness. *Biology,* 11 (5): 719-733.

Dong, T., Ye, N., Yuan, L., Wu, S., Xia, L. and Fang, B. (2020) Assessing the Influence of Chin Asymmetry on Perceived Facial Esthetics With 3-Dimensional Images. *Journal of Oral Maxillofacial Surgery,* 78 (8): 1389–1396.

Finelle, G. (2017) Digital Design in interdisciplinary and orthodontic dental treatment planning. *Journal of Dentofacial Anomalies and Orthodontics,* 20 (3): 303-322.

Freitas, B.V., Rodrigues, V.P., Rodrigues, M.F., de Melo, H.V.F. and dos Santos, P.C.F. (2019) Soft tissue facial profile changes after orthodontic treatment with or without tooth extractions in Class I malocclusion patients: A comparative study. *Journal of Oral Biology and Craniofacial Research*, 9 (2): 172–176.

Gallardo, Y.N.R., Salazar-Gamarra, R., Bohner, L., De Oliveira, J.I., Dib, L.L. and Sesma, N. (2021) Evaluation of the 3D error of 2 face-scanning systems: An invitro analysis. *The Journal of Prosthetic Dentistry*, 129 (4): 630-636.

Gibelli, D., Pucciarelli, V., Poppa, P., Cummaudo, M., Dolci, C., Cattaneo, C. and Sforza, C. (2018) Three-dimensional facial anatomy evaluation: Reliability of laser scanner consecutive scans procedure in comparison with stereophotogrammetry. *Journal of Cranio-Maxillofacial Surgery*, 46 (10): 1807-1813.

Gibelli, D., Tarabbia, F., Restelli, S., Allevi, F., Dolci, C., Dell'Aversana Orabona, G., Cappella, A., Codari, M., Sforza, C. and Biglioli, F. (2020) Three-dimensional assessment of restored smiling mobility after reanimation of unilateral facial palsy by triple innervation technique. *International Journal of Oral and Maxillofacial Surgery,* 49 (4): 536-542.

Güler, Ö.Ç. and Malkoç, S. (2020) Comparison of facial soft tissue changes after treatment with 3 different functional appliances. *American Journal of Orthodontics and Dentofacial Orthopedics,* 158 (4): 518–526.

Gwilliam, J.R., Cunningham, S.J. and Hutton, T. (2006) Reproducibility of soft tissue landmarks on three-dimensional facial scans. *European Journal of Orthodontics*, 28 (5): 408–415.

Hajeer, M.Y., Ayoub, A.F., Millett, D.T. (2004) Three-dimensional assessment of facial soft-tissue asymmetry before and after orthognathic surgery. *British Journal of Oral and Maxillofacial Surgery*, 42 (5): 396-404.

van der Heide, U. A., Frantzen-Steneker, M., Astreinidou, E., Nowee, M.E. and van Houdt, P.J. (2019) MRI basics for radiation oncologists. *Clinical and Translational Radiation Oncology*, 18: 74-79.

Heike, C.L., Upson, K., Stuhaug, E. and Weinberg, S.M. (2010) 3D digital stereophotogrammetry: A practical guide to facial image acquisition. *Head and Face Medicine*, 6: 1–11.

Hell, B. (1995) 3D Sonography, *International Journal of Oral and Maxillofacial Surgery*, 24 (1): 84–89.

ter Horst, R., Maal, T.J.J., de Koning, M.J.J., Mertens, J.S., Schatorjè, E.J.H., Hoppenreijs, E.P. and Seyger, M.M.B. (2022) 3D stereophotogrammetry in children and adolescents with Scleroderma En Coup De Sabre/Parry-Romberg Syndrome: Description of a novel method for monitoring disease progression. *Skin Health and Disease,* 2 (3): 132-139.

Houston, W.J.B. (1983) The analysis of errors in orthodontic measurements. *American Journal of Orthodontics*, 83 (5): 382-390.

Hsu, C-K., Hallac, R.R., Denadai, R., Wang, S-W., Kane, A.A., Lo, L-J. and Chou, P-Y. (2019) Quantifying normal head form and craniofacial asymmetry of elementary school students in Taiwan. *Journal of Plastic, Reconstructive & Aesthetic Surgery*, 72 (12): 2033–2040.

Hull, R.H. (2016) The art of nonverbal communication in practice. *The Hearing Journal*, 69 (5): 22-24.

Jabar, N., Robinson, W., Goto, T.K. and Khambay, B. (2015) The validity of using surface meshes for evaluation of three-dimensional maxillary and mandibular surgical changes. *International Journal of Oral and Maxillofacial Surgery*, 44 (7): 914–920.

Jablonski, R.Y., Osnes, C.A., Khambay, B., Nattress, B.R. and Keeling, A.J. (2019) Accuracy of capturing oncology facial defects with multimodal image fusion versus laser scanning. *Journal of Prosthetic Dentistry*, 122 (3): 333-338.

Johnston, D.J., Millett, D.T., Ayoub A.F. and Bock, M. (2003) Are Facial Expressions Reproducible? *Cleft Palate-Craniofacial Journal,* 40 (3): 291-296.

Jreige, C.S., Kimura, R.C., Coelho Segundo, A.R.T., Coachman, C. and Sesma N. (2022) Esthetic treatment planning with digital animation of the smile dynamics: A technique to create a 4-dimensional virtual patient. *The Journal of Prosthetic Dentistry,* 128 (2) 130-138.

Ju, X., O'Leary, E., Peng, M., Al-Anezi, T., Ayoub, A. and Khambay, B. (2016) Evaluation of the Reproducibility of Nonverbal Facial Expressions Using a 3D Motion Capture System. *The Cleft Palate Craniofacial Journal*, 53 (1): 22-9.

Karatas, O. H. and Toy, E. (2014) Three-dimensional imaging techniques: A literature review. *European Journal of Dentistry*, 8 (1): 132-140.

Kawano, Y. (1987) Three dimensional analysis of the face in respect of zygomatic fractures and evaluation of the surgery with the aid of Moiré topography. *Journal of Cranio-Maxillofacial Surgery,* 15: 68-74.

Khambay, B., Lowney, C.J., Hsung, T-C. and Morris, D.O. (2019) Fluctuating asymmetry of dynamic smiles in normal individuals. *International Journal of Oral and Maxillofacial Surgery*, 48 (10): 1372-1379.

Khambay, B., Nairn, N., Bell, A., Miller, J., Bowman, A. and Ayoub A.F. (2008) Validation and reproducibility of a high-resolution three-dimensional facial imaging system. *British Journal of Oral and Maxillofacial Surgery*, 46 (1): 27-32.

Khambay, B., Nebel, J-C., Bowman, J., Walker, F., Hadley, D.M., and Ayoub, A. (2002) 3D stereophotogrammetric image superimposition onto 3D CT scan images: the future of orthognathic surgery. A pilot study. *The International journal of adult orthodontics and orthognathic surgery*, 17 (4): 331–341.

Knoops, P.G.M., Beaumont, C.A.A., Borghi, A., Rodriguez-Florez, N., Breakey, R.W.F., Rodgers, W., Angullia, F., Jeelani, N.U.O., Schievano, S. and Dunaway, D.J. (2017) Comparison of three-dimensional scanner systems for craniomaxillofacial imaging. *Journal of Plastic, Reconstructive and Aesthetic Surgery*, 70 (4): 441–449.

Kovacs, L., Zimmermann, A., Brockmann, G., Gühring, M., Baurecht, H., Papadopulos, N.A., Schwenzer-Zimmer, K., Sader, R., Biemer, E. and Zeilhofer, H.F. (2006) Three-dimensional recording of the human face with a 3D laser scanner. *Journal of Plastic, Reconstructive & Aesthetic Surgery*, 59 (11): 1193–1202.

Kurnik, N.M., Calis, M., Sobol, D.L., Kapadia, H., Mercan, E. and Tse, R.W. (2021) A comparative assessment of nasal appearance following nasoalveolar molding and primary surgical repair for treatment of unilateral cleft lip and palate. *Plastic and Reconstructive Surgery*, 148 (5): 1075–1084.

Kusnoto, B., Evans, C.A. and Chicago, D.M.S. (2002) Reliability of a 3D surface laser scanner for orthodontic applications. *American Journal of Orthodontics and Dentofacial Orthopedics,* 122 (4): 342-348.

Lane, C. and Harrell, W. (2008) Completing the 3-dimensional picture. *American Journal of Orthodontics and Dentofacial Orthopedics*, 133 (4): 612–620.

Li, J., Zhou, J. and Zhang, J. (2015) A novel dynamical 3D smile measurement method to evaluate the effects of face-lifting surgery: Based on the optical structured light strategy. *Optik,* 126 (18): 1716-1719.

Liu, J., Zhang, C., Cai, R., Yao, Y., Zhao, Z. and Liao, W. (2021) Accuracy of 3-dimensional stereophotogrammetry: Comparison of the 3dMD and Bellus3D facial scanning systems with one another and with direct anthropometry. *American Journal of Orthodontics and Dentofacial Orthopedics*. 160 (6): 862–871.

van Loon, B., Maal, T.J., Plooij, J.M., Ingels, K.J., Borstlap, W.A., Kuijpers-Jagtman, A.M., Spauwen, P.H., Berge, S.J. (2010) 3D Stereophotogrammetric assessment of pre- and postoperative volumetric changes in the cleft lip and palate nose. *International Journal of Oral and Maxillofacial Surgery*: 39 (6): 534–540.

Lübbers, H.T., Medinger, L., Kruse, A., Grätz, K.W. and Matthews, F. (2010) Precision and accuracy of the 3dmd photogrammetric system in craniomaxillofacial application. *Journal of Craniofacial Surgery*, 21 (3): 763–767.

Lum, V., Goonewardene, M.S., Mian, A. and Eastwood, P. (2020) Three-dimensional assessment of facial asymmetry using dense correspondence, symmetry, and midline analysis. *American Journal of Orthodontics and Dentofacial Orthopedics*, 158 (1): 134–146.

Ma, L., Xu, T. and Lin, J. (2009) Validation of a three-dimensional facial scanning system based on structured light techniques. *Computer Methods and Programs in Biomedicine*, 94 (3): 290–298.

Machado, G. L. (2015) CBCT imaging – A boon to orthodontics. *The Saudi Dental Journal*, 27 (1): 12–21.

Menéndez López-Mateos, M.L., Carreño-Carreño, J., Palma, J.C., Alarcón, J.A., Menéndez López-Mateos, C. and Menéndez-Núñez, M. (2019) Three-dimensional photographic analysis of the face in European adults from southern Spain with normal occlusion: Reference anthropometric measurements. *BMC Oral Health,* 19 (1): 1–8.

Metzler, P., Geiger, E.J., Chang, C.C., Sirisoontorn, I. and Steinbacher, D.M. (2014) Assessment of three-dimensional nasolabial response to Le Fort I advancement. *British Journal of Plastic Surgery*, 67 (6): 756–763.

Meulstee, J. W., de Jong, G.A., Borstlap, W.A., Koerts, G., Maal, T.J.J. and Delye, H. (2020) The normal evolution of the cranium in three dimensions. *International Journal of Oral and Maxillofacial Surgery*, 49 (6): 739–749.

Millsopp L., Brandom, L., Humphris, G., Lowe, D., Stat, C. and Rogers, S. (2006) Facial appearance after operations for oral and oropharyngeal cancer: a comparison of casenotes and patient-completed questionnaire. *British Journal of Oral and Maxillofacial Surgery*, 44 (5): 358-63.

Ngan, D.C.S., Kharbanda, O.P., Geenty J.P., Darendeliler, D.M. (2003) Comparison of radiation levels from computed tomography and conventional dental radiographs. *Australiasian Orthodontic Journal*, 19 (2): 67–75.

Nord, F., Ferjencik, R., Seifert, B., Lanzer, M., Gander, T., Matthews, F., Rücker, M. and Lübbers, H.T. (2015) The 3dMD photogrammetric photo system in cranio-maxillofacial surgery: Validation of interexaminer variations and perceptions. *Journal of Cranio-Maxillofacial Surgery*, 43 (9): 1798–1803.

Pan, F., Liu, J., Cen, Y., Chen, Y., Cai, R., Zhao, Z., Liao, W. and Wang, J. (2022) Accuracy of RGB-D camera-based and stereophotogrammetric facial scanners: a comparative study. *Journal of dentistry*, 127: 104302.

Piedra-Cascón, W., Meyer, M.J., Methani, M.M. and Revilla-León, M. (2020) Accuracy (trueness and precision) of a dual-structured light facial scanner and interexaminer reliability. *Journal of Prosthetic Dentistry*, 124 (5): 567-574.

Porto, F., Gurgel, J.L., Russomano, T., and De Tarso Veras Farinatti, P. (2010) Moiré topography: Characteristics and clinical application. *Gait and Posture*, 32 (3): 422–424.

Raffone, C., Gianfreda, F., Bollero, P., Pompeo, M.G., Miele, G. and Canullo, L. (2022) Chairside virtual patient protocol. Part 1: Free vs Guided face scan protocol. *Journal of Dentistry,* 116: 103881.

Ritschl, L.M., Roth, M., Fichter, A.M., Mittermeier, F., Kuschel, B., Wolff, K-D., Grill, F. and Loeffelbein, D.J. (2018) The possibilities of a portable low-budget three-dimensional stereophotogrammetry system in neonates: a prospective growth analysis and analysis of accuracy. *Head & Face Medicine,* 14 (1): 1–11.

Rongo, R., Nissen, L., Leroy, C., Michelotti, A., Cattaneo, P.M. and Cornelis, M.A. (2021) Dimensional soft tissue changes in orthodontic extraction and non-extraction patients: A prospective study. *Orthodontics and Craniofacial Research,* 24 (2): 181–192.

Sawyer, A.R., See, M. and Nduka, C. (2009) Assessment of the reproducibility of facial expressions with 3-D stereophotogrammetry. *Otolaryngology – Head and Neck Surgery,* 140 (1): 76-81.

Shepperson, A. (2023) The Digital Aesthetic Drive. *Primary Dental Journal*, 12 (2): 46-56.

Smith, O.A.M., Nashed, Y.S.G., Duncan, C., Pears, N., Profico, A. and O'Higgins, P. (2021) 3D Modelling of craniofacial ontogeny and sexual dimorphism in children. *The Anatomical Record,* 304 (9): 1918–1926.

Sun, W., Xu, M. and Song, T. (2022) Landmark movement trajectory: A simple reference to understand the dominant muscle contraction in a dynamic smile expression. *Journal of Plastic, Reconstructive & Aesthetic Surgery,* 75 (7): 2310-2316.

Tanikawa, C. and Takada, K. (2018) Test-retest reliability of smile tasks using three-dimensional facial topography. *Angle Orthodontist,* 88 (3): 318-328.

Thierens, L.A.M., De Roo, N.M.C., De Pauw, G.A.M. and Brusselaers, N. (2018) Assessment modalities of non-ionizing three-dimensional images for the quantification of facial morphology, symmetry, and appearance in cleft lip and palate: a systematic review. *International Journal of Oral and Maxillofacial Surgery*, 47 (9): 1095–1105.

Thurzo, A., Strunga, M., Havlínová, R., Reháková, K., Urban, R., Surková, J. and Kurilovà, V. (2022) Smartphone-Based Facial Scanning as a Viable Tool for Facially Driven Orthodontics? *Sensors*, 22 (20): 7752.

Ubaya, T., Sherriff, A., Ayoub, A. and Khambay, B. (2012) Soft tissue morphology of the naso-maxillary complex following surgical correction of maxillary hypoplasia. *International Journal of Oral and Maxillofacial Surgery,* 41 (6): 727-732.

Wampfler, J.J. and Gkantidis, N. (2022) Superimposition of serial 3-dimensional facial photographs to assess changes over time: A systematic review. *American Journal of Orthodontics and Dentofacial Orthopedics*, 161 (2): 182-197.

Wang, C., Shi Y-F., Xiong, Qian., Xie, P-J., Wu, J-H. and Liu, W-C. (2022) Trueness of One Stationary and Two Mobile Systems for Three-Dimensional Facial Scanning. *The International Journal of Prosthodontics,* 35 (3): 350-356.

Wang, J., An, Y-X., Shi, Y-L., Liu, L-P., Zhao, Y-Q., Wu, F. and Wei, H-B. (2022) A digital workflow to predict facial aesthetics in patients with maxillofacial trauma with implant retained prostheses. *Journal of Prosthodontic Research*. Advanced publication.

Winder, R. J., Darvann, T.A., McKnight, W., Magee, J.D.M and Ramsay-Baggs, P. (2008) Technical validation of the Di3D stereophotogrammetry surface imaging system. *British Journal of Oral and Maxillofacial Surgery*, 46 (1): 33–37.

Wong, J.Y., Oh, A.K., Ohta, E., Hunt, A.T., Rogers, G.F., Mulliken, J.B. and Deutsch, C.K. (2008) Validity and reliability of craniofacial anthropometric measurement of 3D digital photogrammetric images. *Cleft Palate-Craniofacial Journal*, 45 (3): 232–239.

Yuen, K., Inokuchi, I., Maeta, M., Kawakami, S-I. and Madusa, Y. (1997) Evaluation of facial palsy by moirè topography index. *Otolaryngology – Head and Neck Surgery,* 117 (5): 567-572.

Zachrisson, B.U. (1998) Esthetic factors involved in anterior tooth display and the smile: vertical dimension. *Journal of Clinical Orthodontics,* 32: 432-445.

Zammit-Maempel, I. (2015) Imaging of the head and neck. *Surgery,* 33 (12): 627–632.

Zhou, Q., Gao, J., Guo, D., Zhang, H., Zhang, X., Qin, W. and Jin, Z. (2023) Three dimensional quantitative study of soft tissue changes in nasolabial folds after orthodontic treatment in female adults. *BMC Oral Health*, 23: 31

CHAPTER 8

APPENDICES

8.1 Appendix I Consent form

UNIVERSITY OF BIRMINGHAM | SCHOOL OF DENTISTRY

Version 1 / 25th March 2019

Centre Number:
Study Number:
Identification Number for this trial:

CONSENT FORM
Title of project: Validity of a Tablet based device for 3D facial capture
Name of Researcher: Professor Balvinder Khambay

Please initial box

1. I confirm I have read and understand the information sheet dated 25th March 2019 (version 1.1) for the above study. I have had the opportunity to consider the information, ask questions and have had these answered satisfactorily. ☐
2. I understand that my participation is voluntary and that I am free to withdraw my data within 12 weeks of participation without giving any reason, without my legal rights being affected. ☐
3. I agree to take part in the above study. ☐
4. I understand that data from this study may be used in future research. ☐

----------	----------	----------
Name of volunteer	Date	Signature

----------	----------	----------
Name of Person taking consent	Date	Signature

Validity of a Tablet based device for 3D facial capture		
Consent sheet	Version 1	25th March 2019

8.2 Appendix II Volunteer information sheet

UNIVERSITY OF BIRMINGHAM | SCHOOL OF DENTISTRY

The title of the research project
Validity of a Tablet based device for 3D facial capture

Invitation paragraph
You are being invited to take part in a research project. Before you decide, it is important for you to understand why the research is being done and what it will involve. Please take time to read the following information carefully and discuss it with others if you wish. Ask us / me if there is anything that is not clear or if you would like more information. Take time to decide whether or not you wish to take part.

What is the purpose of the project?
To see if a new Tablet based device (Bellus3D) can capture your face in 3D. At present we use an expensive non-mobile camera system (3dMD system), located at the Birmingham Dental Hospital, to routinely photograph patients. We are hoping the Bellus3D Tablet based system will be able to replace the 3dMD. This will allow more research to be carried out in other hospitals.

3dMD system

Bellus3D

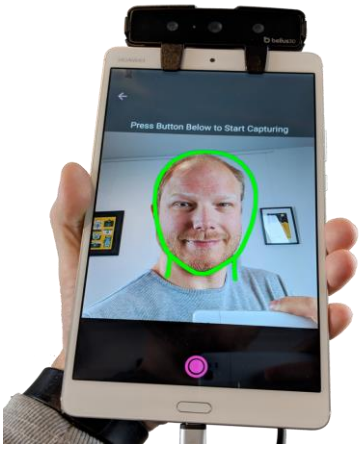

Why have I been chosen?
We are looking for 50 volunteers between the ages of 18 and 50.

What do I have to do and what will happen to me if I take part?
You will be asked to attend the Birmingham Dental Hospital & School for a period of approximately 30 minutes.

We will place around 35 dots on your face using an eye-linear pencil (washes off afterwards) and take a 3D image of your face at rest and smiling using both the 3dMD system and the Bellus3D system.

In addition we will mould some modeling clay material onto your face to work out how well Bellus3D can measure volume. We will take images of your face at rest, with and without the modeling clay on your face, using both the 3dMD system and Bellus3D Tablet.

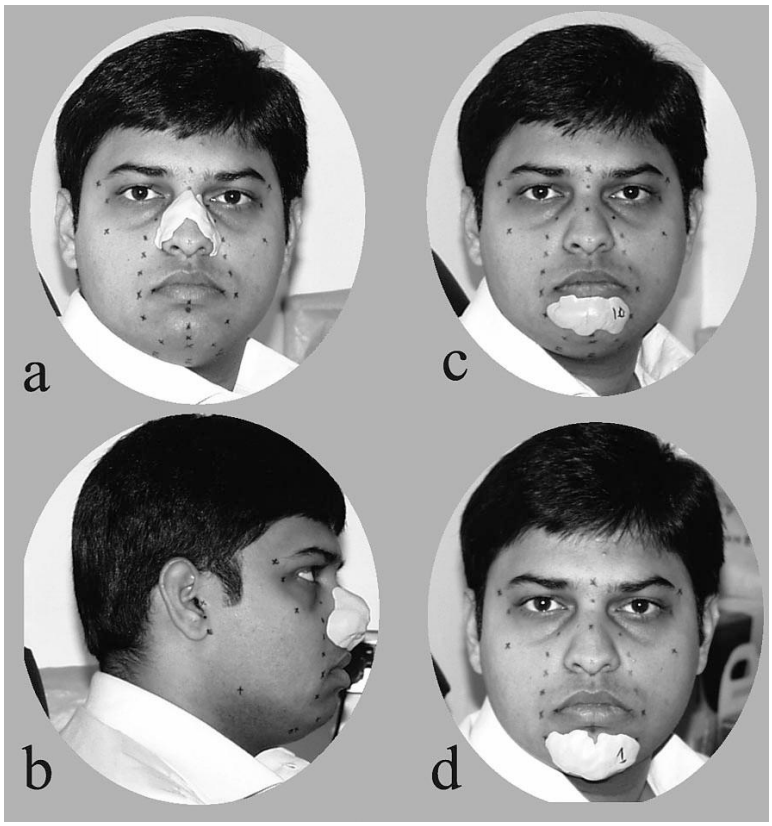

From: Hajeer MY, Mao Z, Millett DT, Ayoub AF, Siebert JP. A new three-dimensional method of assessing facial volumetric changes after orthognathic treatment. CleftPalate Craniofac J. 2005 Mar;42(2):113-20.

It is up to you to decide whether or not to take part. If you do decide to take part you will be given this information sheet to keep (and be asked to sign a consent form). If you wish to withdraw you can do so without it affecting any benefits that you are entitled to in any way. You do not have to give a reason.

You can withdraw at any time but your data cannot be withdrawn after 12 weeks of completion of the study. We may use your data from this study for future research projects. Your data will be treated in accordance with the Data Protection Act 2018.

Will my taking part in this project be kept confidential and what will happen to the results of the research project?
Yes. Only the researchers involved will know you have taken part. The images generated will not be used in publications unless you have specifically consented. They may however be used in presentations to fellow researchers who are also interested in this technology. Your facial images will not be shown, only the results of the study.

What will happen to the results of the study?
The main findings will be written up and submitted to an appropriate scientific journal; again your facial images will not appear in the journal unless formal approval has been obtained.

Contact for further information

If you have any further queries please do not hesitate to contact any of the researchers involved via the email addresses supplied above.

Professor Balvinder Khambay
Tel
Email:

This study has been reviewed and given a favourable opinion by University of Birmingham, Research Ethics Committee on the 25th March 2019 and ethics reference ERN_19-0165.